

Quantum many-body scars as remnants of stable many-body periodic orbits

Keita Omiya

PSI Center for Scientific Computing, Theory and Data, 5232 Villigen PSI,
Switzerland

Institute of Physics, Ecole Polytechnique Fédérale de Lausanne (EPFL),
CH-1015 Lausanne, Switzerland

October 24, 2024

Abstract

Quantum many-body scars (QMBS) represent a weak ergodicity-breaking phenomenon that defies the common scenario of thermalization in closed quantum systems. They are often regarded as a many-body analog of quantum scars (QS)—a single-particle phenomenon in quantum chaos—due to their superficial similarities. However, unlike QS, a clear connection between QMBS and classical chaos has remained elusive. It has nevertheless been speculated that in an appropriate semiclassical limit, QMBS should have a correspondance to weakly unstable periodic orbits. In this paper, I present a counterexample to this conjecture by studying a bosonic model with a large number of flavors. The dynamics of out-of-time-ordered correlators (OTOCs) suggest that QMBS do not display chaotic behavior in the semiclassical limit. In contrast, chaotic dynamics are expected for initial states not associated with QMBS. Interestingly, the anomalous OTOC dynamics persist even under weak perturbations that eliminate the scarred eigenstates, suggesting a certain robustness in the phenomenon.

1 Introduction and summary

The question of thermalization in closed quantum many-body systems is one of the central problems in statistical physics. Although it remains an open problem requiring extensive study, the Eigenstate Thermalization Hypothesis (ETH) [1, 2] is a widely accepted concept. The ETH posits that the expectation values evaluated in each eigenstate of a generic many-body system should coincide with that evaluated in the corresponding Gibbs ensemble in the thermodynamic limit. This hypothesis has been tested and confirmed primarily through numerical simulations across various systems, e.g., in Ref [3].

However, Ref. [4] points out that thermalization does not necessarily imply the ETH. In fact, Ref. [4] outlines a systematic method of constructing non-integrable models which violate the ETH while still allowing for thermalization for almost all initial states, with the exception of a vanishing fraction of initial states that do not thermalize. This construction is known as the Shiraishi-Mori (SM) construction. The core idea is that an ETH-violating subspace, characterized as the common kernel of local projectors, is embedded within the many-body Hilbert space, and the interaction is fine-tuned such that this subspace remains invariant under the Hamiltonian. The Hamiltonian from this construction typically takes the form $H = \sum_{\alpha} P_{\alpha} h_{\alpha} P_{\alpha} + H_Z$ with P_{α} a local projector characterizing the subspace and H_Z a trivially integrable term (such as a Zeeman term) that preserves the special subspace. A straightforward consequence of the SM construction is that if the initial state is a superposition of eigenstates within the ETH-violating subspace, it will either (i) avoid thermalization or (ii) reach a stationary state that is not described by the standard Gibbs ensemble [5].

A remarkable experiment involving an array of Rydberg atoms [6] is believed to approximately realize the scenario (i). In this experiment, anomalous oscillations persisted much longer than the typical timescale of the system, but only when the initial state was the \mathbb{Z}_2 -ordered state. A common interpretation of these oscillations is that the initial \mathbb{Z}_2 state is approximately a superposition of ETH-violating eigenstates, also known as scar states [7], which possess an almost equidistant energy spectrum, yielding quasi-periodic motions that assures slow thermalization.

This phenomenon was termed quantum many-body scars (QMBS) in Ref. [7] due to its resemblance to the single-particle phenomenon known as quantum scars (QS) in quantum billiards [8]. A QS is a significant quantum correction to the Wigner function, leading to the concentration of certain atypical “scarred” eigenfunctions on classical unstable periodic orbits. This phenomenon provides a counterexample to Berry’s conjecture asserting that the Wigner function of eigenstates in classically chaotic systems should be delocalized across the whole phase space allowed by symmetries. As a result, an initial Gaussian wavepacket also exhibits long-lasting oscillations, even in a chaotic billiard when placed on weakly unstable periodic orbits.

Despite this loose analogy, the theory of QMBS has largely developed independently of the background known from QS. Numerous toy models, including the spin-1 XY model, have been proposed and analyzed, exhibiting similar phenomenology to the Rydberg experiment [9, 10, 11]. Many of these toy models share common features, which led to several studies attempting a unified construction of those Hamiltonians [12, 13]. One such feature is that the toy models can typically be decomposed into a Zeeman term and a sum of local terms, each of which annihilates the scar states. This structure was found to be a special case of the SM construction. Furthermore, even for the models previously thought to evade such an algebraic characterization, it has been shown that they can be cast into the form of the SM construction once the Hilbert space is properly chosen [14, 15].

While the algebraic aspects of QMBS have been intensively studied, their connection to QS and classical chaos is little understood, partly due to the lack of a parameter interpolating between the available quantum toy models and an appropriate classical limit. Such quantum models consist of quantum spins or fermions, which do not have well-defined classical limits. One possible approach to studying chaos in such systems is to use the time-dependent variational principle (TDVP), where the stability of a specific variational solution can be

examined. Another approach is to move beyond such models and consider semiclassical systems, where chaos can be directly studied by solving the classical equation of motion. The former approach has been employed in the analysis of the PXP model [16], the effective model describing the Rydberg experiment, where the scar states are relatively well understood. However, this approach can only access the stability of the variational manifold, which may differ from that of the quantum state itself. The latter approach is more suited to studying chaos of the system [17, 18, 19], but underlying scar states, if any, are usually difficult to obtain, and one typically relies on numerics that might suffer from finite-size effects. Nevertheless, a prevailing conjecture posits that the proper classical limit of QMBS corresponds to classically unstable periodic orbits.

In this paper, I will show a clear distinction between QMBS and classical chaos using the out-of-time ordered correlator (OTOC) [20, 21] (the precise definition is given in Eq. (2.6) in Sec. 2). More precisely, I will compute OTOCs for a generic chaotic single-particle system and a simple many-body system hosting QMBS originating from an SM-like structure. The early time behavior of the OTOC of an unstable periodic orbit in the single-particle system exhibits conventional Lyapunov growth,

$$OTOC(t) \sim \hbar^2 \# e^{2\lambda_L t}, \quad (1.1)$$

where λ_L is the Lyapunov exponent (LE) calculated classically. Here, the small parameter of the theory is \hbar . It is particularly important that the exponent λ_L is a quantity of order $O(1) = O(\hbar^0)$. In contrast, the OTOC of the periodic orbit originating from the scar states does not exhibit such rapid growth. The early time behavior is instead given by

$$OTOC(t) \sim \frac{\#}{N} e^{\lambda t/N}, \quad (1.2)$$

where $1/N$, the inverse of the number of flavor degrees of freedom, is the small parameter of the theory. The semiclassical limit corresponds to $N \rightarrow \infty$, and thus the LE vanishes in this limit. Note that, similar to the QS scenario, the periodic orbit corresponds to a periodic solution of the classical equation of motion in the large- N limit. Therefore, Eq. (1.2) implies that the periodic orbit is destabilized solely by quantum fluctuation. The (classically) vanishing LE turns out to be a distinctive feature of QMBS in this model. The model further hosts another classically unstable periodic orbit that is, however, not associated with a QMBS. The OTOC of this orbit satisfies the conventional form like Eq. (1.1),

$$OTOC(t) \sim \frac{\#}{N} e^{2\lambda_L t}, \quad (1.3)$$

where λ_L is an $O(1)$ quantity calculated from the quadratic action. Eqs. (1.1-1.3) indicate clearly the different behavior of the two periodic orbits.

Another important question in the study of QMBS is the stability of scarring under perturbations to the Hamiltonian. Many existing toy models feature finely tuned algebraic structures that facilitate scarring, yet the effects of perturbations that disrupt these structures remain less understood. Given that these models are inherently non-integrable and often strongly interacting, studies on the fate of QMBS under perturbations have primarily relied on numerical simulations of small system sizes or perturbative analysis [22, 23, 24, 25]. The

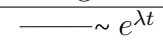
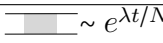
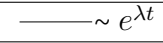

System	Parameter	$OTOC(t)$	Mechanism	Diagram
QS (Sec. 3)	\hbar	$\sim e^{O(t)}$	Quadratic	
QMBS (Sec. 5)	$1/N$	$\sim e^{O(t/N)}$	Second order	
Generic orbit (Sec. 6)	$1/N$	$\sim e^{O(t)}$	Quadratic	
Perturbed QMBS (Sec. 7)	$1/N$	subexponential	First order	

Table 1: Summary of the different behaviors of the OTOCs and their origin.

model in this paper provides a novel insight beyond these common approaches: when a perturbation disrupts the SM structure of the Hamiltonian, the scar states cease to be exact eigenstates. The behavior of the OTOC is modified differently depending on perturbation strength: when the coupling constant is smaller than a certain threshold, indicating a weak perturbation, it is modified as,

$$OTOC(t) \sim \frac{\#}{N} C(t), \quad (1.4)$$

where $C(t)$ is a sub-exponential function with an $O(1)$ value. Eq. (1.4) implies that although the weak scar-breaking perturbation destabilizes the periodic orbit, the conventional Lyapunov growth is still absent. On the other hand, when the perturbation is larger than the threshold, the OTOC shows conventional exponential growth like Eq. (1.1) or Eq. (1.3).

The difference in behavior of the OTOCs originates from the SM structure. The monodromy matrix of an unstable periodic orbit typically has at least one eigenvalue with a positive real part, leading to the destabilization of the periodic orbit. In cases where the monodromy matrix has only pure imaginary eigenvalues (note that for Hamiltonian systems, the sum of the eigenvalues must be zero), linear stability analysis is inconclusive, necessitating consideration of higher-order terms. However, stability analysis beyond linearization is challenging and often requires a case-by-case approach. Remarkably, the SM structure guarantees that higher-order terms do not destabilize the periodic orbit in the semiclassical limit. Therefore only quantum fluctuations can destabilize the orbit, implying the LE of order $1/N$. Once the weak scar-breaking perturbation is added, the monodromy matrix still does not show unstable modes while higher-order terms affect the periodic orbit, eventually destabilizing it. This implies that OTOCs do grow, but their growth is subexponential.

The rest of the paper is organized as follows. Sec. 2 provides a concise overview of the basic concepts and technical tools utilized in this study. In Sec. 3, I calculate the OTOC for a generic single-particle system, under the assumption of classical chaos, and demonstrate conventional Lyapunov growth of the OTOC, with the LE calculated obtained from classical calculations [Eq. (1.1)]. Sec. 4 introduces the many-body model, where I examine its thermodynamic properties and highlight an observable that indicates a violation of the ETH. The analysis of the scar states within this model is presented in Sec. 5, where the LE is derived via the Bethe-Salpeter (BS) equation, revealing its disappearance in the semiclassical limit. Sec. 6 identifies another periodic orbit within the model, showing that the corresponding OTOC exhibits conventional Lyapunov growth. The impact of perturbation that breaks the scar structure is addressed in Sec. 7. There I show that while the system exhibits chaotic dynamics even in the large- N limit, conventional Lyapunov growth remains absent. The paper concludes with a summary and final remarks in Sec. 8.

2 Preliminaries

2.1 Shiraishi-Mori construction of many-body scars

This paper focuses on the SM construction, one of the simplest methods for generating models that host QMBS. Other approaches, such as spectrum generating algebra (SGA) [26], are reviewed in Ref. [27]. Consider a Hamiltonian of the form:

$$H = \sum_i P_i h_i P_i + H', \quad (2.1)$$

where P_i is a projector and h_i is an arbitrary Hermitian operator. If there exists at least one state $|\psi\rangle$ that is annihilated by all projectors P_i , i.e., $P_i |\psi\rangle = 0 \forall i$, then the “scar subspace” $\mathcal{V}_{\text{scar}}$ can be defined as the common kernel of P_i . If $\mathcal{V}_{\text{scar}}$ is invariant under H' , the Hamiltonian H will have $N_{\text{scar}} = \dim \mathcal{V}_{\text{scar}}$ eigenstate(s) $|S_n\rangle$ within the scar subspace, i.e., $|S_n\rangle \in \mathcal{V}_{\text{scar}}$ ($n = 1 \sim N_{\text{scar}}$). The eigenstate(s) should satisfy the condition $\langle S_n | P_i | S_n \rangle = 0$ by construction, violating the ETH since the thermal expectation value of P_i at any non-zero temperature is strictly positive.

A natural extension of Eq. (2.1) is to replace the projector with an operator that has a non-empty kernel. In this work, I set $P_i = b_i$, where b_i is a bosonic annihilation operator. Consequently, the scar states satisfy the condition $\langle S_n | b_i^\dagger b_i | S_n \rangle = 0$. This extension, however, does not necessarily guarantee violation of the ETH. The infinite dimensionality of the local Hilbert space in bosonic systems and the unbounded nature (in terms of an operator norm) of local terms in the Hamiltonian invalidate the key technical ingredient of the proof of the ETH violation. To address this, I consider the large- N limit, where the model becomes classical and exactly solvable. In this regime, the expectation value of $b_i^\dagger b_i$ can be directly calculated, demonstrating ETH violation. Although this approach does not rigorously prove ETH violation for finite N , the thermal expectation value $\langle b_i^\dagger b_i \rangle$ should be close to its large- N limit, with deviations of order $1/N$.

2.2 Lyapunov exponent in out-of-time order correlator

The OTOC was first introduced in the context of dirty superconductors in Ref. [20], and later gained prominence for its role in studying quantum chaos, particularly in studying blackhole scrambling [28], and the conjectured chaos bound [29]. In classical mechanics, the LE λ_L describes the exponential divergence of trajectories, captured by the Poisson bracket of observables at different times,

$$\{x(t), p(0)\}_{\text{P.B.}} = \frac{\partial x(t)}{\partial x(0)} \sim e^{\lambda_L t}, \quad (2.2)$$

where $\{A, B\}_{\text{P.B.}}$ is the Poisson bracket. In quantum mechanics, the Poisson bracket is replaced by the commutator ($\{, \}_{\text{P.B.}} \mapsto (i\hbar)^{-1}[\ ,]$), and the square of this operator defines the OTOC:

$$\text{OTOC}(t) = \langle [x(t), p(0)][x(t), p(0)]^\dagger \rangle, \quad (2.3)$$

where $x(t)$ and $p(0)$ are now operators. The bracket represents the quantum mechanical average (see below for the precise definition used in this paper). From Eq. (2.2) one expects

$OTOC(t) \sim \hbar^2 e^{2\lambda t}$. More generally, the OTOC can be defined for any pair of operators V and W :

$$OTOC(t) = \langle [V(t), W(0)][V(t), W(0)]^\dagger \rangle. \quad (2.4)$$

In the case of mixed states, there is some ambiguity in defining the expectation value. For instance, “unregularized” and “regularized” OTOCs are often distinguished as follows,

$$\text{Tr}(\rho[V(t), W(0)][V(t), W(0)]^\dagger), \quad \text{Tr}(\sqrt{\rho}[V(t), W(0)]\sqrt{\rho}[V(t), W(0)]^\dagger). \quad (2.5)$$

These different definitions can lead to different prefactors in the OTOC [30]. Throughout this paper, however, all OTOCs are computed with respect to pure states. Specifically, I use the following definition of the OTOC relative to a reference state $|\psi\rangle$,

$$OTOC(t) = \langle \psi|[V(t), W(0)][V(t), W(0)]^\dagger|\psi\rangle. \quad (2.6)$$

3 Lyapunov growth in a single-particle semiclassical system

In this section I study an OTOC of a single-particle semiclassical chaotic system and demonstrate that it exhibits conventional Lyapunov growth. Quantum scarring refers to the concentration of eigenfunctions on classically unstable periodic orbits in semiclassical billiards [31]. A single-particle wavepacket initialized on a weakly unstable periodic orbit exhibits anomalously long-lasting oscillations before eventually spreading out across the entire system [8]. These oscillations suggest the existence of scarred eigenstates. Following this approach, I consider a chaotic single-particle system described by the Hamiltonian $H = p^2/2m + U(x)$ where in the classical limit, the equation of motion admits an unstable periodic orbit with period T . Here the operators x and p satisfy the canonical commutation relation $[x, p] = i\hbar$ with \hbar treated as a small parameter. Unlike the original setting of quantum scarring, where $U(x)$ represents the sharp boundary of a billiard, I assume that the confining potential $U(x)$ is a smooth function of x . To compute the OTOC, I introduce the ladder operator,

$$a = \sqrt{\frac{m\Omega}{2}}x + i\frac{p}{\sqrt{2m\Omega}}, \quad (3.1)$$

where $\Omega = 2\pi/T$. This operator satisfies the commutation relation $[a, a^\dagger] = \hbar$, and I denote the normal ordered Hamiltonian as

$$H = \sum_{n=0}^{\infty} \hbar^n H_n(a^\dagger, a). \quad (3.2)$$

$H_n(n \geq 1)$ is obtained by normal ordering the original Hamiltonian, and thus in the semiclassical limit ($\hbar \rightarrow 0$) it should vanish. The classical equation of motion is recovered by neglecting correlations (e.g., $\langle a^n \rangle \approx \langle a \rangle^n$) of H_0 . The equation for $\langle a \rangle$ within this approximation is written as

$$i\frac{d\langle a \rangle}{dt} \approx \frac{\partial H_0(\langle a^\dagger \rangle, \langle a \rangle)}{\partial \langle a^\dagger \rangle}, \quad (3.3)$$

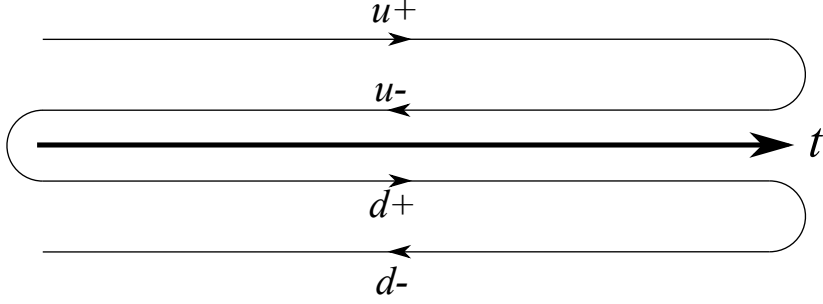


Figure 1: Two folded Keldysh contour. The arrows indicate the path-ordering of operators in the Keldysh formalism.

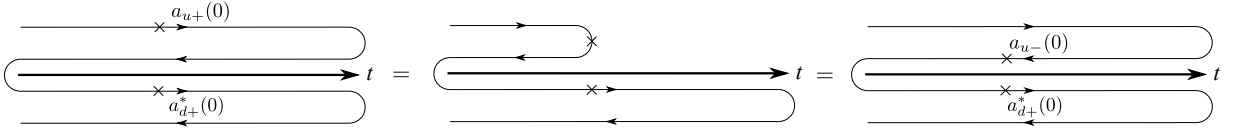


Figure 2: A graphical proof of the equality $\langle a_{d+}^*(0)a_{u-}(0) \rangle = \langle a_{d+}^*(0)a_{u+}(0) \rangle$ (the first line of Eq. (3.10)). Due to the unitarity, part of the $(u+)$ - and $(u-)$ -branches can be cancelled out, allowing the Keldysh contour to be folded immediately after time 0.

which is equivalent to the classical equation of motion, or the Ehrenfest theorem. By assumption Eq. (3.3) has a periodic solution, which I denote $\alpha_0(t)$. The stability of this solution can be inspected by checking the eigenvalues of the monodromy matrix $M(t)$, which is the Hessian of H_0 with respect to the periodic solution. Namely, $M(t)$ is defined as

$$M(t) = \begin{pmatrix} \frac{\partial^2 H_0}{\partial(a^\dagger)\partial(a)} & \frac{\partial^2 H_0}{\partial(a^\dagger)\partial(a^\dagger)} \\ \frac{\partial^2 H_0}{\partial(a)\partial(a)} & \frac{\partial^2 H_0}{\partial(a)\partial(a^\dagger)} \end{pmatrix} \Big|_{((a), (a^\dagger)) = (\alpha_0(t), \alpha_0^*(t))}. \quad (3.4)$$

I will compute the following OTOC $C(t)$,

$$C(t) = \theta(t) \langle g|[a(t), a^\dagger(0)][a(t), a^\dagger(0)]^\dagger|g \rangle, \quad (3.5)$$

where $|g\rangle$ is a Gaussian wavepacket centered on the periodic orbit. In the following I will sketch the important steps of the derivation, and leave details in Appendix A. $C(t)$ can be computed perturbatively with the small parameter \hbar . Technically this perturbative expansion should be carried out in the two-folded Keldysh contour (Fig. 1), as Eq. (3.5) is not time-ordered. However this is not necessary in order to obtain the LE only to the leading order in \hbar as shown below.

To compute Eq. (3.5) I define the retarded Green's function G^R ,

$$iG^R(t, 0) = \theta(t) \langle g|[a(t), a^\dagger(0)]|g \rangle. \quad (3.6)$$

G^R can be computed perturbatively with respect to \hbar : in this approach the unperturbed part of the Hamiltonian corresponds to the monodromy matrix $M(t)$ and all the other terms

are regarded as perturbations. Note that G^R directly enters the OTOC: for example, at the zeroth order of Eq. (3.5) is a product of G^R ,

$$C^{(0)}(t) = G_0^R(t, 0)(G_0^R(t, 0))^*, \quad (3.7)$$

where $G_0^R(t, 0)$ is the bare Green's function. Since this form will appear frequently in subsequent OTOC computations, here I provide a detailed derivation: the OTOC is decomposed as

$$C(t) = \theta(t) \left(\langle g|a(t)a^\dagger(0)a(0)a^\dagger(t)|g \rangle - \langle g|a(t)a^\dagger(0)a^\dagger(t)a(0)|g \rangle \right) - \theta(t) \left(\langle g|a^\dagger(0)a(t)a(0)a^\dagger(t)|g \rangle - \langle g|a^\dagger(0)a(t)a^\dagger(t)a(0)|g \rangle \right). \quad (3.8)$$

These four-point functions can be written as products of two-point functions by Wick theorem. For instance, within the zeroth order in the perturbation theory, the first two terms in Eq. (3.8) in the path-integral formalism are written as

$$\begin{aligned} \langle g|a(t)a^\dagger(0)a(0)a^\dagger(t)|g \rangle &= \langle a_{d-}(t)a_{d+}^*(0)a_{u-}(0)a_{u+}^*(t) \rangle \\ &= \langle a_{d-}(t)a_{d+}^*(0) \rangle \langle a_{u-}(0)a_{u+}^*(t) \rangle + \langle a_{d-}(t)a_{u+}^*(t) \rangle \langle a_{d+}^*(0)a_{u-}(0) \rangle \\ &\quad + \langle a_{d-}(t)a_{u-}(0) \rangle \langle a_{d+}^*(0)a_{u+}^*(t) \rangle \\ \langle g|a(t)a^\dagger(0)a^\dagger(t)a(0)|g \rangle &= \langle a_{d-}(t)a_{d+}^*(0)a_{u-}^*(t)a_{u+}(0) \rangle \\ &= \langle a_{d-}(t)a_{d+}^*(0) \rangle \langle a_{u-}^*(t)a_{u+}(0) \rangle + \langle a_{d-}(t)a_{u+}(0) \rangle \langle a_{d+}^*(0)a_{u-}^*(t) \rangle \\ &\quad + \langle a_{d-}(t)a_{u+}^*(t) \rangle \langle a_{d+}^*(0)a_{u+}(0) \rangle, \end{aligned} \quad (3.9)$$

where the right-hand side (RHS) represents the path-integral formulation with the bosonic fields a_γ, a_γ^* ($\gamma = (u\pm), (d\pm)$) residing in the γ -branch of the Keldysh contour. The unitarity of the time-evolution permits deformations of the Keldysh contour, leading to the following identities (see Fig. 2 for the graphical representation),

$$\begin{aligned} \langle a_{d+}^*(0)a_{u-}(0) \rangle &= \langle a_{d+}^*(0)a_{u+}(0) \rangle \\ \langle a_{d-}(t)a_{u-}(0) \rangle &= \langle a_{d-}(t)a_{u+}(0) \rangle \\ \langle a_{d+}^*(0)a_{u+}^*(t) \rangle &= \langle a_{d+}^*(0)a_{u-}^*(t) \rangle. \end{aligned} \quad (3.10)$$

Substituting these equalities into Eq. (3.9), the first line of the RHS in Eq. (3.8) takes the following simple form,

$$\begin{aligned} &\theta(t) \left(\langle g|a(t)a^\dagger(0)a(0)a^\dagger(t)|g \rangle - \langle g|a(t)a^\dagger(0)a^\dagger(t)a(0)|g \rangle \right) \\ &= \theta(t) \langle a_{d-}(t)a_{u+}^*(0) \rangle \langle (a_{u-}(0)a_{u+}^*(t) - a_{u-}^*(t)a_{u+}(0)) \rangle \\ &= \theta(t) \langle a_{d-}(t)a_{u+}^*(0) \rangle \left(\langle g|[a(t), a^\dagger(0)]|g \rangle \right)^* \\ &= -i\theta(t) \langle a_{d-}(t)a_{d+}^*(t) \rangle (G_0^R(t, 0))^*. \end{aligned} \quad (3.11)$$

The same procedure can be applied to the second line of Eq. (3.8), yielding Eq. (3.7).

As shown in Appendix A, calculation of the bare Green's function is equivalent to finding the eigenmodes of the monodromy matrix,

$$i\sigma^3 \frac{d\psi_\alpha(t)}{dt} = M(t)\psi_\alpha(t), \quad (3.12)$$

where $\sigma^3 = \text{diag}(1, -1)$ is the Pauli matrix. Since $M(t)$ is periodic in time, the Floquet theorem applies and $\psi_\alpha(t)$ is written as $\psi_\alpha(t) = e^{\lambda_\alpha t} u_\alpha(t)$ where $u_\alpha(t)$ is a periodic function. The exponential factor with the largest real part ($\max_\alpha \text{Re } \lambda_\alpha$) corresponds to the (classical) LE of the periodic orbit. Note that Eq. (3.7) already shows the exponential growth: using the normal modes $\psi_\alpha(t)$, the OTOC is written as,

$$C^{(0)}(t) = \hbar^2 \theta(t) \left| \sum_\alpha e^{\lambda_\alpha t} [u_\alpha(t) u_\alpha^\dagger(0)]_{11} \right|^2, \quad (3.13)$$

where $[A]_{11}$ indicates the (1, 1)-component of the matrix A .

Eq. (3.13) and Eq. (3.12) show that, to the leading order (in \hbar), the OTOC is equivalent to the classical problem, i.e., finding the eigenmodes of the monodromy matrix. I emphasize that in this case the Lyapunov exponent $\text{Re } \lambda_\alpha$ is $O(1)$, which is not affected by the semiclassical limit ($\hbar \rightarrow 0$). For QMBS the situation is rather different. In Sec. 5, I will show that the OTOC for QMBS at the leading order does not show any exponential divergence, and only quantum corrections are responsible for the Lyapunov growth of the OTOC, which implies that in the semiclassical limit they vanish.

4 Many-body model and thermodynamics

I consider a one-dimensional N -flavor bosonic system with periodic boundary conditions,

$$\begin{aligned} H &= H_0 + V \\ H_0 &= -t \sum_{i=1}^L \sum_{\mu=1}^N (a_{i\mu}^\dagger a_{i+1\mu} + a_{i+1\mu}^\dagger a_{i\mu} + b_{i\mu}^\dagger b_{i+1\mu} + b_{i+1\mu}^\dagger b_{i\mu}) + \mu \sum_{i=1}^L \sum_{\mu=1}^N (a_{i\mu}^\dagger a_{i\mu} + b_{i\mu}^\dagger b_{i\mu}) \\ &\equiv \sum_{k \in \text{BZ}} \sum_{\mu=1}^N \xi_k (a_{k\mu}^\dagger a_{k\mu} + b_{k\mu}^\dagger b_{k\mu}) \\ V &= \sum_{i=1}^L v_i, \end{aligned} \quad (4.1)$$

where $a_{i\mu}$ ($a_{k\mu}$) and $b_{i\mu}$ ($b_{k\mu}$) are bosonic annihilation operators at the site i (in momentum space) and $\xi_k = -2t \cos k + \mu > 0$ is a dispersion. The local potential, v_i , is defined as

$$v_i = \frac{J}{N^2} \sum_{\mu, \nu, \rho=1}^N :b_{i\mu}^\dagger b_{i\mu} (a_{i\nu} + a_{i\nu}^\dagger)^2 (b_{i\rho} + b_{i\rho}^\dagger)^2:, \quad (4.2)$$

where $:\bullet:$ is the normal order and J is set positive. The prefactor J/N^2 is chosen so that the potential energy is proportional to N ($\langle v_i \rangle = O(N)$). This model has a parameter N , the number of flavors, and in the large- N limit the saddle-point (or the mean-field) approximation becomes exact. Therefore $1/N$ plays the role of \hbar in QS, and for this reason I set $k_B = \hbar = 1$.

This model hosts exponentially many scar states, as shown in Sec. 5. They consist solely of a -bosons and thus annihilated by each local potential v_i since v_i must contain at least one annihilation operator of b -bosons. The absence of b -bosons implies that the scar states are not thermal, as discussed below.

Before proceeding with the analysis of this model, a few preliminary remarks are necessary. The specific form of the interaction v_i does not appear to be crucial; different potentials should yield similar OTOC behavior to those summarized in Table 1, as long as each term v_i annihilates the scar states defined in Eq. (5.1) in Sec. 5, i.e., the SM structure described in Sec. 5 is preserved. However, it is preferable to choose a potential that is lower-bounded, and explicitly breaks the $U(1)$ symmetry of a - and b -bosons. For bosonic models, lower-bounded potentials are generally required so that the free energy is lower-bounded. Since the OTOCs defined in Eq. (5.6) and Eq. (6.6) below correspond to perturbations of periodic orbits by adding a single boson, maintaining $U(1)$ symmetry could significantly constrain the phase space the system can explore, potentially suppressing chaos (see also the discussion following Eq. (5.6) in Sec. 5). As discussed below, the model can be considered a simple deformation in that the potential v_i only breaks the system's $U(1)^{2N}$ symmetry of the non-interacting part.

4.1 Spontaneous symmetry breaking

While this model does not possess the full $U(1)$ symmetry of a - and b -bosons, it has an $O(N)^2$ symmetry, which is represented by the following action,

$$\begin{aligned} \frac{a_{i\mu} + a_{i\mu}^\dagger}{2} &\rightarrow \sum_{\nu=1}^N U_{\mu\nu} \frac{a_{i\nu} + a_{i\nu}^\dagger}{2}, & \frac{a_{i\mu} - a_{i\mu}^\dagger}{2i} &\rightarrow \sum_{\nu=1}^N U_{\mu\nu} \frac{a_{i\nu} - a_{i\nu}^\dagger}{2i} \\ \frac{b_{i\mu} + b_{i\mu}^\dagger}{2} &\rightarrow \sum_{\nu=1}^N V_{\mu\nu} \frac{b_{i\nu} + b_{i\nu}^\dagger}{2}, & \frac{b_{i\mu} - b_{i\mu}^\dagger}{2i} &\rightarrow \sum_{\nu=1}^N V_{\mu\nu} \frac{b_{i\nu} - b_{i\nu}^\dagger}{2i}, \end{aligned} \quad (4.3)$$

where U and V are distinct elements of $O(N)$. The symmetry of the zero-temperature state is studied by the Euler-Lagrange (EL) equation for $a_\mu = \langle a_{i\mu} \rangle$, $b_\mu = \langle b_{i\mu} \rangle$, which reads,

$$\begin{aligned} E a_\mu + 2J \left(\frac{1}{N} \sum_{\nu=1}^N |b_\nu|^2 \right) \left(\frac{1}{N} \sum_{\rho=1}^N (b_\rho + b_\rho^*)^2 \right) (a_\mu + a_\mu^*) &= 0 \\ E b_\mu + J \left(\frac{1}{N} \sum_{\nu=1}^N (a_\nu + a_\nu^*)^2 \right) \left[\left(\frac{1}{N} \sum_{\rho=1}^N (b_\rho + b_\rho^*)^2 \right) b_\mu + \left(\frac{2}{N} \sum_{\rho=1}^N |b_\rho|^2 \right) (b_\mu + b_\mu^*) \right] &= 0, \end{aligned} \quad (4.4)$$

where $E = -2t + \mu$ is the dispersion at $k = 0$. The first line implies $a_\mu \in \mathbb{R}$, as the second term is real so that the equation is written as $A a_\mu = B$ with $A, B \in \mathbb{R}$. This in turn implies $b_\mu \in \mathbb{R}$ by a similar reasoning. The reality of a_μ and b_μ simplifies Eq. (4.4) further as

$$\begin{aligned} \left(E + 16J \left(\frac{1}{N} \sum_{\nu=1}^N b_\nu^2 \right)^2 \right) a_\mu &= 0 \\ \left(E + 32J \left(\frac{1}{N} \sum_{\nu=1}^N a_\nu^2 \right) \left(\frac{1}{N} \sum_{\rho=1}^N b_\rho^2 \right) \right) b_\mu &= 0. \end{aligned} \quad (4.5)$$

When $E > 0$, Eq. (4.5) has the unique solution $a_\mu = b_\mu = 0$. When $E < 0$, which will however not be relevant for the subsequent discussion, the solution of Eq. (4.5) is

$$\frac{1}{N} \sum_{\mu=1}^N a_\mu^2 = \frac{1}{8} \sqrt{\frac{-E}{J}}, \quad \frac{1}{N} \sum_{\mu=1}^N b_\mu^2 = \frac{1}{4} \sqrt{\frac{-E}{J}}, \quad (4.6)$$

which breaks the $O(N)^2$ symmetry.

4.2 Mean-field analysis: equilibrium

Since the Euclidean action of the model S_E is proportional to N , the saddle-point (or mean-field) approximation becomes exact in the large- N limit. In this limit, the thermal expectation value of an observable O is simply given by the saddle-point value,

$$\begin{aligned} \lim_{N \rightarrow \infty} \langle O \rangle &\equiv \lim_{N \rightarrow \infty} \int D[a^*, a] D[b^*, b] D\Delta_a Dv_a D\Delta_b Dv_b O e^{-S_E} \\ &= \lim_{N \rightarrow \infty} \int D[a^*, a] D[b^*, b] O e^{-S_E^*}, \end{aligned} \quad (4.7)$$

where $\Delta_{a/b}$ and $v_{a/b}$ are auxiliary fields that make the action quadratic in a and b (see Appendix B for the detailed discussion), and S_E^* is obtained by substituting the saddle-point value of the auxiliary fields into S_E .

Within the mean-field approximation, one can show that the density of the b -bosons (see Appendix B),

$$\rho_b = \frac{1}{NL} \sum_{i=1}^L \sum_{\mu=1}^N b_{i\mu}^\dagger b_{i\mu}, \quad (4.8)$$

has to be strictly positive for any T , i.e., $\langle \rho_b \rangle_T > 0$. In Sec. 5 below I will define the scar states [Eq. (5.1)], and show that they are characterized by the property $\rho_b |\psi\rangle = 0$, meaning that the scar states cannot be thermal eigenstates at any T .

Strictly speaking, the treatment in this section is insufficient to prove violation of the ETH in a rigorous manner: the positivity of ρ_b at any temperature can be shown only for the large- N limit, while OTOCs are computed for large but finite N . However, it is reasonable to assume that the difference between the finite N and the large- N results is subleading in N and thus $\langle \rho_b \rangle_T$ should still be strictly positive.

5 Scar states and Lyapunov exponent

Any state containing solely a -bosons is annihilated by each local potential v_i as $b_i \in v_i$. This type of construction of the scarred Hamiltonian can be viewed as a variant of the SM construction since the scar subspace is a common kernel of each local operator v_i . In the present case, the following Fock space \mathcal{F}_a is the scar subspace,

$$\mathcal{F}_a = \text{span} \left\{ \prod_{k \in \text{BZ}} \prod_{\mu=1}^N (a_{k\mu}^\dagger)^{n_{k\mu}} |0\rangle \mid n_{k\mu} \in \mathbb{Z}_{\geq 0} \right\}, \quad (5.1)$$

where $|0\rangle$ is the vacuum state. Within \mathcal{F}_a , only the non-interacting part of the Hamiltonian acts non-trivially. As a result, the Fock states of a -bosons in the momentum basis are exact eigenstates. This structure is common in many toy models of QMBS, where the Hamiltonian is typically a sum of a Zeeman term and locally annihilating terms. Any state $|\psi\rangle$ in \mathcal{F}_a violates ETH since $\langle \psi | \rho_b | \psi \rangle = 0$ while the thermal expectation value is strictly positive at any temperature. A simple consequence of the existence of the scar states is the failure of thermalization when the system is initialized within the scar subspace, i.e., a state containing only the a -boson. Specifically let us consider the following coherent state $|\alpha\rangle$ as the initial state,

$$a_{i\mu} |\alpha\rangle = \alpha_\mu |\alpha\rangle, \quad b_{i\mu} |\alpha\rangle = 0 \quad \forall i, \mu. \quad (5.2)$$

This state will never thermalize. The time-evolution is given by a simple precession of the coherent state,

$$|\alpha(t)\rangle = |\alpha e^{-iEt}\rangle, \quad E = -2t + \mu \quad (\forall N). \quad (5.3)$$

Indeed, the Heisenberg equations projected onto \mathcal{F}_a read,

$$i \frac{d \langle \alpha | a_{i\mu}(t) | \alpha \rangle}{dt} = E \langle \alpha | a_{i\mu}(t) | \alpha \rangle, \quad i \frac{db_{i\mu}(t)}{dt} = 0, \quad (5.4)$$

without any approximation. In the Keldysh path-integral formalism, the solution ($a_{i\mu}(t) = e^{-iEt} \alpha_\mu$ and $b_{i\mu}(t) = 0$) satisfies the EL equation of the Keldysh action (see Eq. (C4) in Appendix C). Note that the energy of this state is conserved and expressed as,

$$\frac{\langle \alpha(t) | H | \alpha(t) \rangle}{NL} = \frac{E}{N} \sum_{\mu=1}^N |\alpha_\mu|^2 \equiv E\alpha^2. \quad (5.5)$$

Recall that $E = -2t + \mu > 0$. The energy of the state $|\alpha(t)\rangle$ corresponds to that of a high temperature state if α^2 is sufficiently large, as I will assume in what follows.

To study quantum chaos around the scar state $|\alpha(t)\rangle$, I will compute the following OTOC $C_\alpha(t)$,

$$C_\alpha(t) = \frac{\theta(t)}{N^2} \sum_{i=1}^L \sum_{\mu, \nu=1}^N \langle \alpha | [b_{i\mu}(t), b_{j\nu}^\dagger(0)] [b_{i\mu}(t), b_{j\nu}^\dagger(0)]^\dagger | \alpha \rangle. \quad (5.6)$$

The choice of the operators for OTOC is motivated by the following observation: let $C_{VW}(t)$ be the OTOC with respect to the operators V and W ,

$$C_{VW}(t) = \frac{\theta(t)}{N^2} \sum_{i=1}^L \sum_{\mu, \nu=1}^N \langle \alpha | [V(t), W(0)] [V(t), W(0)]^\dagger | \alpha \rangle, \quad (5.7)$$

where the above choice [Eq. (5.6)] corresponds to $V = b, W = b^\dagger$. One can immediately find that the choice $V = a, W = a^\dagger$ (or $V = a^\dagger, W = a$) does not show any chaos, as the dynamics is closed within the scar subspace. Another choice $V = a, W = b^\dagger$ does not reveal any information of the system either, since

$$C_{a, b^\dagger}(t) = \frac{\theta(t)}{N^2} \sum_{i=1}^L \sum_{\mu, \nu=1}^L \langle \alpha | a(t) b^\dagger b a^\dagger(t) | \alpha \rangle = 0, \quad (5.8)$$

due to the property of the scar states $b|\psi\rangle = 0$. While the choice $V = b, W = a^\dagger$ does lead to exponential growth of the OTOC, the exponent is smaller than the one in $C_\alpha(t)$ when α is large enough. Therefore, I will compute the particular choice of the OTOC, i.e., $C_\alpha(t)$ as it is expected to exhibit the largest LE.

The $U(1)$ -breaking interaction [Eq. (4.2)] is expected to favor chaoticity by lifting symmetry-related restrictions. The dynamics of the system would be otherwise restricted, as the reference state $|\alpha\rangle$ does not contain any b -bosons. Specifically, the dimension of the Fock space of one-particle b -boson states \mathcal{F}_b^1 , which would constitute the accessible part of the Hilbert space to the system if $U(1)$ were preserved, is NL ($\dim \mathcal{F}_b^1 = NL$). This is significantly smaller than the typical dimension of the many-body Hilbert space within the energy shell corresponding

to a given finite temperature, which scales as $e^{O(NL)}$. In the following I will demonstrate that, even without such entropic protection, QMBS exhibit considerable stability due to the underlying SM structure.

Following equilibrium cases [32, 33], $C_\alpha(t)$ is calculated by the perturbation theory in the interaction J in the two-folded Keldysh contour (Fig. 1). Since the calculation is lengthy but not worth inspecting except for Eq. (5.17) and Eq. (5.22), I will present only the important steps and results, and leave details in Appendix. C.

5.1 Retarded Green's function

I first calculate the retarded Green's function G^R up to the second order in J . G^R is defined as

$$iG^R(k; t, t') = \theta(t - t') \langle \alpha | [b_{k\mu}(t), b_{k\mu}^\dagger(t')] | \alpha \rangle. \quad (5.9)$$

Note that due to the permutation symmetry of the Hamiltonian, one can omit the flavor index μ . As in Sec. 3, G^R directly enters the expression of the OTOC: for example, at the zeroth order of J , it is written as,

$$C_S^{(0)}(t) = \frac{1}{NL} \sum_{k \in \text{BZ}} G_0^R(k; t, 0) (G_0^R(k; t, 0))^*, \quad (5.10)$$

where G_0^R is the bare Green's function. One can derive Eq. (5.10) in a similar manner to Eq. (3.7).

5.1.1 The first order correction

The first order perturbation corresponds to the diagram shown in the left panel of Fig. 3. Furthermore, when all the corresponding higher corrections are taken into account, one arrives at the Hartree diagram, the right panel of Fig. 3. This correction usually yields the mean-field equation. However, it is important that these corrections vanish for the scar states. As one can read from the diagram, the corrections contain normal ordered quadratic terms $\langle b_k^\dagger(t) b_k(t) \rangle$, $\langle b_{-k}(t) b_k(t) \rangle$, and $\langle b_k^\dagger(t) b_{-k}^\dagger(t) \rangle$, which are always zero since b_k annihilates the scar states.

The vanishing the Hartree term turns out to be the most important characteristics of the (exact) scar states: as in the single-particle case in Sec. 3, bare Green's functions exhibit exponential divergence for generic unstable periodic orbits. This is also true for the present model, as discussed in Sec. 6. In rare cases where bare Green's functions do not diverge exponentially, *full* Green's functions are still expected to diverge, although such divergence may be subexponential. The absence of exponential divergence in bare Green's functions and subexponential growth in full Green's functions are indeed observed when a weak perturbation is added, as discussed in Sec. 7. On the other hand, the amplitude of even the full Green's function of the exact QMBS remains constant in the semiclassical limit ($N \rightarrow \infty$). Moreover, as shown below, the absence of growth in the Green's function persists even when quantum corrections (up to order $1/N$) are taken into account.



Figure 3: The Feynman diagram of the first order perturbation (left) and the Hartree diagram (right). Only these contributions will survive in the large- N limit, However, the both diagrams vanish for the scar state. Once the scar-breaking perturbation is added, these diagrams affect the dynamics (see Sec. 7).

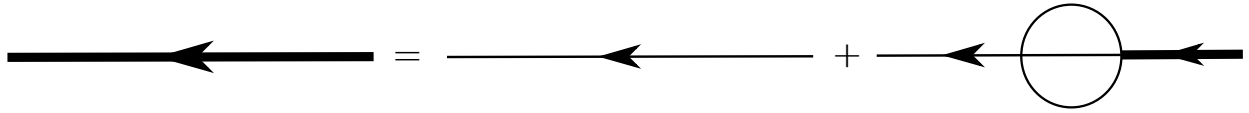


Figure 4: A graphical representation of the Dyson equation. Since the Hartree diagram should always vanish due the property of the scar state $b_{i\mu}(t)|\alpha\rangle = 0$, it consists only of second order perturbations (up to $1/N$).

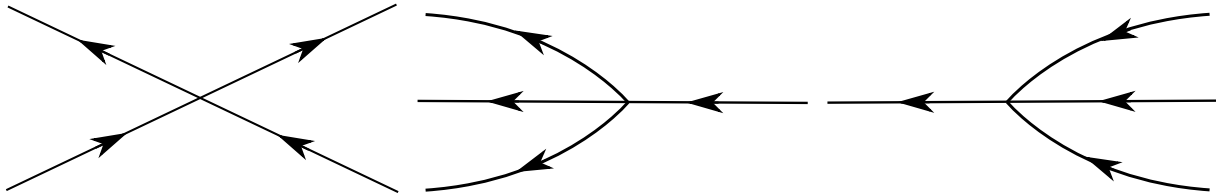


Figure 5: Three scattering processes relevant for the second order corrections to the Green's function: the number conserving two-body scattering (left), the number increasing scattering (middle), and the number decreasing scattering (right).

5.1.2 The second order correction

The second order corrections correspond to the self-energy that is order $1/N$. The Dyson equation is

$$G^R(t, t') = G_0^R(t, t') - \int_{-\infty}^{\infty} dt_1 dt_2 G_0^R(t, t_1) \Sigma(t_1, t_2) G^R(t_2, t'). \quad (5.11)$$

Under the assumption that α^2 is sufficiently large, the dominant contribution to Σ is written as,

$$\Sigma(t_1, t_2) \approx \frac{8J^2\alpha^4}{N} \cos^2(Et_1) \cos^2(Et_2) \tilde{\Sigma}[G_0], \quad (5.12)$$

where $\tilde{\Sigma}[G_0]$ is a functional of the bare Green's function defined in Eq. (C8) in Appendix C. Note that for the early time Lyapunov growth of the OTOC, it is sufficient to consider the self-energy consisting of the bare Green's functions $\tilde{\Sigma}[G_0]$, instead of the full Green's function ($\tilde{\Sigma}[G]$). In the momentum space the Dyson equation becomes

$$G^R(k, \omega) = G_0^R(k, \omega) - G_0^R(k, \omega) \sum_{n \in \mathbb{Z}} \Sigma_n(k, \omega) G^R(k, \omega + 2nE), \quad (5.13)$$

which resembles the Schrödinger equation of periodically driven systems. Indeed, the $2nE$ shift of the frequency comes from the cosines, the effect of the periodic orbit. While the exact solution of Eq. (5.13) seems formidable, a perturbative calculation is still possible, and it is sufficient to determine the LE up to the order of $1/N$.

Eq. (5.13) can be written in vector form,

$$\begin{pmatrix} \vdots \\ G^R(k, \omega - 2E) \\ G^R(k, \omega) \\ G^R(k, \omega + 2E) \\ \vdots \end{pmatrix} = \begin{pmatrix} \vdots \\ G_0^R(k, \omega - 2E) \\ G^R(k, \omega) \\ G^R(k, \omega + 2E) \\ \vdots \end{pmatrix} - G_0^R(k) \Sigma(k) \begin{pmatrix} \vdots \\ G^R(k, \omega - 2E) \\ G^R(k, \omega) \\ G^R(k, \omega + 2E) \\ \vdots \end{pmatrix}, \quad (5.14)$$

where

$$G_0^R(k) = \text{diag}(\dots, G_0^R(k, \omega - 2E), G_0^R(k, \omega), G_0^R(k, \omega + 2E), \dots)$$

$$\Sigma(k) = \begin{pmatrix} \ddots & & & & & & \\ \dots & \Sigma_{-1}(k, \omega) & \Sigma_0(k, \omega) & \Sigma_{+1}(k, \omega) & \dots & & \\ & \dots & \Sigma_{-1}(k, \omega + 2E) & \Sigma_0(k, \omega + 2E) & \Sigma_{+1}(k, \omega + 2E) & \dots & \\ & & & & & \ddots & \\ & & & & & & \ddots \end{pmatrix}. \quad (5.15)$$

I decompose the “matrix” Σ as the diagonal part D_Σ and the non-diagonal part N_Σ , i.e., $\Sigma = D_\Sigma + N_\Sigma$. Eq. (5.13) is formally solved by inverting the matrix $1 + G_0^R \Sigma$, and the effect of the non-diagonal part can be incorporated perturbatively,

$$(1 + G_0^R(k) \Sigma(k))^{-1} = (1 + G_0^R(k) D_\Sigma(k))^{-1} + \sum_{n=1}^{\infty} ((1 + G_0^R(k) D_\Sigma(k))^{-1} N_\Sigma(k))^n (1 + G_0^R(k) D_\Sigma(k))^{-1}. \quad (5.16)$$

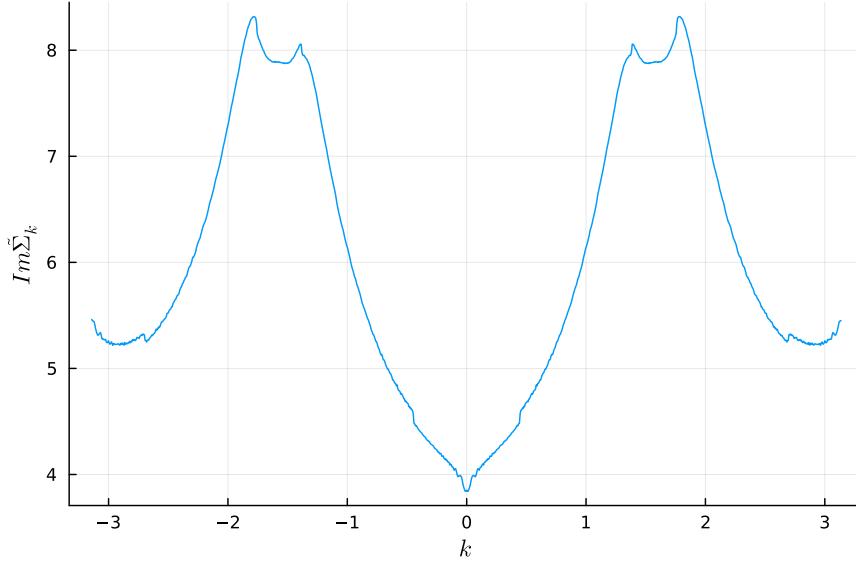


Figure 6: The imaginary part of the rescaled self-energy $\tilde{\Sigma}_k$ for each wavevector $k \in [-\pi, \pi]$. For the parameters I set $\xi_k = -2 \cos k + 2.5$ and $L = 2^{10}$. The infinitesimal number 0^+ in the definition of the retarded Green's function is set $0^+ = 3/2^{10}$.

Since each component of \mathbf{N}_Σ is of order $1/N$ (recall that $\Sigma(t_1, t_2)$ in Eq. (5.12) is proportional to $1/N$), it is sufficient to consider the first line in the RHS of Eq. (5.16) for determining the Lyapunov exponent up to the order of $1/N$,

$$G^R(k, \omega) \approx \frac{1}{\omega - \xi_k + \Sigma_0(k, \omega)} \approx \frac{1}{\omega - \xi_k + \Sigma_k}, \quad (5.17)$$

where the self-energy correction Σ_k is defined in Eq. (C10) or Eq. (C12) in Appendix C.

Note that the imaginary part of Σ_k is more relevant than the real part for the LE since the real part merely yields a frequency shift. The expression of $\text{Im} \Sigma_k$ in Eq. (C12) shows that three scattering processes are relevant to the self-energy correction, and they represent either decay or amplification of the quasiparticles (Fig. 5): the two-body scattering (the left diagram in Fig. 5) and the number increasing scattering (the middle diagram in Fig. 5) induce decay of the quasiparticles, while the number decreasing scattering (the right diagram in Fig. 5) might cause a dynamical instability. However, the numerical integration of $\text{Im} \Sigma_k$ shown in Fig. 6 indicates that the first two processes are always dominant. In Fig. 6, I plot the rescaled self-energy $\tilde{\Sigma}_k$ defined as,

$$\Sigma_k = \frac{8J^2\alpha^4}{N} \tilde{\Sigma}_k. \quad (5.18)$$

The positivity of $\text{Im} \Sigma_k$ indicates that the quasi-particles always decay, meaning that at the single-particle level no chaos can be observed. This should be contrasted to standard QS's, where the bare Green's function already shows exponential growth.

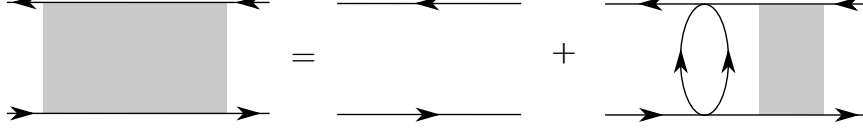


Figure 7: The Feynman diagram of the BS equation for the OTOC. The full correlator is obtained by resumming the “rung” diagram.

5.2 Bethe-Salpeter equation

The absence of leading-order exponential growth in the Green’s function implies that in order to capture the Lyapunov growth of the OTOC, the perturbative calculation requires the two-folded Keldysh contour, which was not necessary for the QS in Sec. 3. One can work out this perturbative expansion to find the following structure: the OTOC is written as,

$$\begin{aligned}
 C_\alpha(t) &= \frac{1}{NL} \sum_{k \in \text{BZ}} f(k; (t, t), (0, 0)) \\
 C_\alpha(\omega) &= \frac{1}{NL} \sum_{k \in \text{BZ}} \int \frac{dk_0}{2\pi} f(k, k_0, \omega),
 \end{aligned} \tag{5.19}$$

where the second line is the Laplace transform of $C_\alpha(t)$. Indeed, at the zeroth order in J (see Eq. (5.10), also see Eq. (C18)) the OTOC satisfies this form by setting $f^{(0)}(k; (t, t), (0, 0)) = G_0^R(t, 0)(G_0^R(t, 0))^*$ and $f(k, \omega) = G_0^R(k, k_0)(G_0^R(k, k_0 - \omega))^*$.

The equation for $f(k; (t, t), (0, 0))$ (Eq. (C19) in Appendix C) is equivalent to the Bethe-Salpeter (BS) equation,

$$\begin{aligned}
 f(k, (t, t), (0, 0)) &= f^{(0)}(k; (t, t), (0, 0)) \\
 &+ \int_0^t dt_1 dt_2 f^{(0)}(k; (t, t), (t_1, t_2)) \sum_{q \in \text{BZ}} R(k, (t_1, t_2); q, (0, 0)) f(q; (t_1, t_2), (0, 0)),
 \end{aligned} \tag{5.20}$$

where R is the “rung diagram” as shown in Fig. 7. More specifically, R is written as,

$$R(k, (t_1, t_2); q, (0, 0)) = \frac{8J^2\alpha^4}{NL^2} \cos^2(Et_1) \cos^2(Et_2) K[G_0^W], \tag{5.21}$$

where $K[G_0^W]$ is a functional of the (bare) Wightman function G_0^W (see Appendix C). One can further assume the on-shell condition $f(k, k_0, \omega) = \delta(k_0 - \xi_k) f(k, \omega)$, which is an analog of the quasiparticle approximation in the Boltzmann equation, and obtain the following linear equation,

$$-i\omega f(k, \omega) \approx -\text{Im} \Sigma_k f(k, \omega) + \sum_{n \in \mathbb{Z}} \sum_{q \in \text{BZ}} K_{-n}(k, q) f(q, \omega + 2nE), \tag{5.22}$$

where the “kernel” K_{-n} is defined in Appendix C. The LE corresponds to the eigenvalue of the RHS of Eq. (5.22). Although solving this eigenvalue problem seems a formidable task, one can perform a similar perturbative calculation for the Green’s function, exact up to order $1/N$. I give the detailed discussion in Appendix C. The upshot is that one needs to only consider K_0 , i.e.,

$$-i\omega f(k, \omega) \approx -\text{Im} \Sigma_k f(k, \omega) + \sum_{q \in \text{BZ}} K_0(k, q) f(q, \omega). \tag{5.23}$$

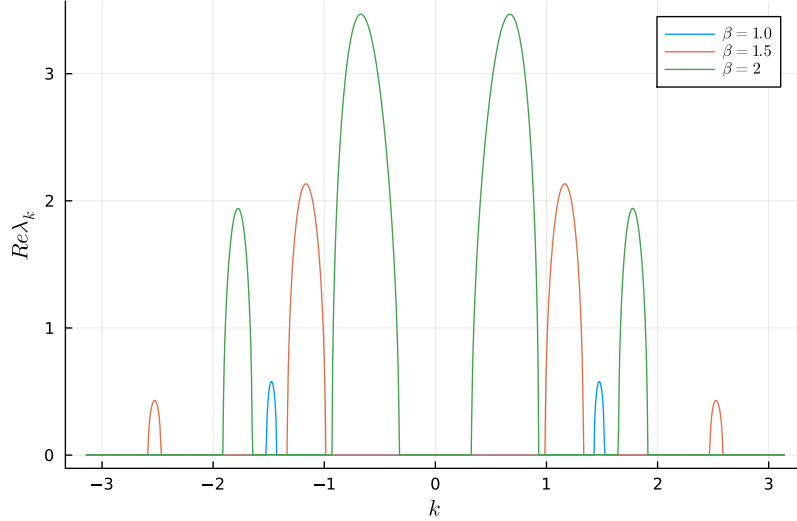


Figure 8: The largest real part of the Lyapunov exponent for each k in the Brillouin zone for different β . $\max_k \text{Re } \lambda_k > 0$ indicates an instability of the periodic orbit. I set $\xi_k = -2 \cos k + 2.5$, $J = 0.1$, and $L = 2^{10}$.

One can numerically compute the maximum eigenvalue of the RHS of Eq. (5.23). For $L = 2^{10}$, $\xi_k = -2 \cos k + 2.5$ I obtain

$$\lambda \approx 0.06567 \frac{J^2 \alpha^4}{N}, \quad (5.24)$$

which is seen to vanish in the semiclassical limit, $N \rightarrow \infty$.

6 Unstable periodic orbit from non-scar states

The classical limit of the model [Eq. (4.1)] hosts further periodic orbits: if one neglects the correlations ($\langle a^2 \rangle \approx \langle a \rangle^2$ etc.), the following function satisfies the Heisenberg equation,

$$\langle a_{i\mu}(t) \rangle = 0, \quad \langle b_{i\mu}(t) \rangle = \beta_\mu e^{-iEt}. \quad (6.1)$$

Unlike the scar state $|\alpha\rangle$ in Sec. 5 where the corresponding solution satisfies the Heisenberg equation exactly, this solution describes approximate oscillations of the phase of b -bosons. Therefore, one expects that Eq. (6.1) should deviate from the exact dynamics after some time, which could be captured by studying an appropriate OTOC. In the following, I will show that this periodic solution is indeed unstable so that the Lyapunov exponent is of order unity.

For this periodic orbit I study the following OTOC $C_\beta(t)$,

$$C_\beta(t) = \frac{\theta(t)}{N^2} \sum_{i=1}^L \sum_{\mu, \nu=1}^N \langle \beta | [a_{i\mu}(t), a_{j\nu}^\dagger(0)] [a_{i\mu}(t), a_{j\nu}^\dagger(0)]^\dagger | \beta \rangle, \quad (6.2)$$

where the state $|\beta\rangle$ corresponds to the classical solution Eq. (6.1),

$$b_{i\mu} |\beta\rangle = \beta_\mu |\beta\rangle, \quad a_{i\mu} |\beta\rangle = 0. \quad (6.3)$$

To compute the OTOC I define the retarded Green's function G^R ,

$$iG^R(k; t, t') = \theta(t - t') \langle \beta | [a_{k\mu}(t), a_{k\mu}^\dagger(t')] | \beta \rangle, \quad (6.4)$$

which appears in the expression of the OTOC to leading order in the perturbation expansion,

$$C_\beta(t) = \frac{\theta(t)}{NL} \sum_{k \in \text{BZ}} G^R(k; t, 0) (G^R(k; t, 0))^*. \quad (6.5)$$

One can follow the same steps as in Sec. 3 and find that the OTOC to the leading order can be written as,

$$C_\beta(t) = \frac{\theta(t)}{NL} \sum_{k \in \text{BZ}} \left| \sum_{\alpha} e^{\lambda_{k\alpha} t} [u_{k\alpha}(t) u_{k\alpha}^\dagger(0)]_{11} \right|^2, \quad (6.6)$$

where $\text{Re } \lambda_{k\alpha} (> 0)$ is the LE of the unstable orbit (see Appendix D for the derivation).

Fig. 8 shows the largest LE $\lambda_k \equiv \max_{\alpha=1,2} \text{Re } \lambda_{k\alpha}$ for $k \in [-\pi, \pi]$ (note the ‘‘band index’’ α introduced in Appendix D). One can recognize several peaks of the LE centered around certain k 's in the Brillouin zone. Those depend on the initial condition $|\beta\rangle$. This structure may be due to resonances between the periodic orbit and the dispersion ξ_k . Since $\max_k \text{Re } \lambda_k > 0$ in all cases, Fig. 8 indicates that the periodic orbits are unstable.

It is important to note that the instability of this periodic orbit comes from the fact that the interaction $\sum_i v_i$ modifies the quadratic part of the Keldysh action such that the renormalized bare Green's function shows a dynamical instability. This should be contrasted to the previously discussed QMBS: due to the property $b_{i\mu}(t) |\psi\rangle = 0$, the interaction does not modify the quadratic action, which makes the LE of the scar state vanish in the semiclassical limit.

7 Effect of a scar-breaking perturbation

Let us introduce the following perturbation to the Hamiltonian,

$$V = -\frac{\epsilon}{2} \sum_{i=1}^L \sum_{\mu=1}^N (b_{i\mu}^2 + (b_{i\mu}^\dagger)^2), \quad (7.1)$$

which disrupts the SM structure. Consequently, the subspace \mathcal{F}_a [Eq. (5.1)] is no longer invariant under the perturbed Hamiltonian, leading to the eventual thermalization of the initial coherent state $|\alpha\rangle$ [Eq. (5.2)]. However, in the mean-field approximation, where the correlations are ignored, the periodic orbit [Eq. (5.2) and Eq. (5.3)] continues to satisfy the equation of motion. In the following, I study the stability of this orbit by computing the same OTOC $C_\alpha(t)$ [Eq. (5.6)].

When the perturbation is sufficiently large, $|\epsilon| > E$, the quadratic component of the Hamiltonian has purely imaginary eigenvalues, indicating a dynamical instability. In this regime, the OTOC can be approximated as:

$$C_\alpha(t) \sim \frac{1}{NL} \sum_{\substack{k \in \text{BZ} \\ \xi_k^2 - \epsilon^2 < 0}} C_k e^{\sqrt{\epsilon^2 - \xi_k^2} t}, \quad (7.2)$$

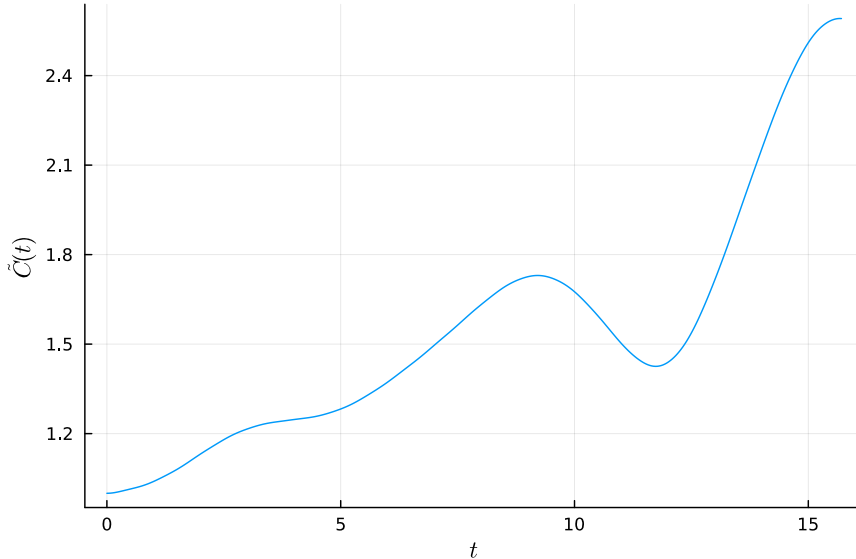


Figure 9: The rescaled OTOC $\tilde{C}(t) = NC_\alpha(t)$. I set $\xi_k = -2 \cos k + 2.5$, $8J\alpha^2 = 3.0$, and $\epsilon = 0.3$.

where C_k is a constant (see Appendix E.1 for the derivation). This mechanism mirrors that of the quasi-periodic motion in QS, where a perturbation alters the quadratic action, rendering certain modes unstable.

For $|\epsilon| < E$, the quadratic action remains non-chaotic. Here, the first-order perturbative effects (Fig. 3) become relevant, unlike for the exact QMBS. Solving the Dyson equation numerically (see Appendix E.2 for the derivation), I find, however, that $C_\alpha(t)$ exhibits non-exponential growth for an early time period (Fig. 9). The absence of conventional Lyapunov growth stems from the fact that the interaction does not modify the quadratic part of the action, emphasizing the role of the non-linearity induced by the higher-order terms. Chaotic dynamics only emerge when higher-order correlations are included.

A couple of brief remarks are in order. First, non-exponential growth of the OTOC under weak perturbations appears to be universal, regardless of the specific form chosen for V . I explored several other simple perturbations that preserve Eq. (5.3) as an approximate solution of the equation of motion, and confirm that none of them leads to exponential OTOC growth. Second, similar subexponential growth has recently been observed in a classical PXP model, where deviations grow only polynomially over time when the initial state is two-site periodic [19]. Since such weakly chaotic dynamics in the classical PXP model may be linked to the anomalous oscillations seen in the Rydberg experiment [6], the mechanism discussed here could offer valuable insight into scarring phenomena beyond solvable toy models.

8 Conclusion

In this paper I discuss a connection between QMBS and classical chaos. The presented model serves as a counterexample to a widely-held conjecture that a proper semiclassical limit of QMBS should involve unstable periodic orbits. Through the lens of OTOCs, I instead demonstrate parametrically long coherent time when the number of flavors N is sufficiently

large. While the OTOC for the periodic orbit of the single-particle billiard system shows the conventional Lyapunov growth, the LE associated with the periodic orbit emanating from the scar states vanishes. Interestingly, this absence of exponential growth persists even under certain weak perturbations. In contrast, periodic orbits that are not connected to the scar states conform with the expected Lyapunov behavior, demonstrating the conventional chaotic dynamics in the classical limit.

The uncovered clear distinction between QMBS and classical chaos aligns with recent studies on a scarring phenomenon in many-body systems [17, 18, 34, 35] and an analysis on the PXP model in semiclassical regime [19]. The former demonstrated that certain eigenstates have enhanced overlap with unstable periodic orbits, while still satisfying the ETH. Therefore, unlike scar states in QMBS, the accurate analogs of the QS in many-body systems are in general thermal. Notably, Srednicki had already pointed out that the ETH is compatible with the QS in his seminal paper [2], and these studies further confirm his insight in many-body contexts. The latter study discovered that a family of classical periodic orbits, which includes the experimentally relevant Néel orbit, is stable, exhibiting pure phase Lyapunov exponents (i.e., $|\lambda| = 1$). This implies that non-chaotic long-lived oscillations in Rydberg atom chains originate from linearly stable periodic orbits, which contrasts sharply with the common speculation [16] that such behaviors should be associated with instability of the periodic orbits.

The suppression of chaotic dynamics of OTOCs in QMBS stems from the SM construction. The interaction annihilates the scar states *locally*, implying the absence of the Hartree term in perturbation theory. As the Hartree is the only possible $O(1)$ contribution in the semiclassical limit $N \rightarrow \infty$, its absence precludes the emergence of chaos in these states. This is a distinctive feature of QMBS, not shared by general periodic orbits in the classical limit, as discussed in Sec. 3 and Sec. 6 where conventional Lyapunov growth is observed. Remarkably, even when a weak scar-breaking perturbation is introduced, the anomalous OTOC dynamics persist, owing to the fact that the quadratic part of the action is not modified by the interaction. However, unlike the exact scar states, the higher-order terms eventually induce chaos, driving the system toward thermalization.

These findings have practical implications for simulating or manipulating QMBS, either in laboratories or in quantum computers [36, 37]. The present model offers a solvable example of a QMBS that remains robust against weak scar-breaking perturbations, at least over a short timescale. Given that QMBS avoid the conventional chaotic dynamics even under a slight perturbation, it is plausible that signatures of QMBS can be detected in realistic systems, which may not perfectly preserve the fine-tuned structures of QMBS due to noise or environmental decoherence. The findings of this paper suggest that the suppression of chaos may be a generic feature of QMBS in the semiclassical limit, including the PXP model. Ref. [19] conducts the stability analysis of a classical PXP model, and finds that conventional Lyapunov growth is absent as well. Confirming the universality of this property in other models is an important step toward understanding the many-body scarring phenomenon.

This study focuses on a weak coupling theory where the quasiparticles are well-defined. It is therefore interesting and worthwhile to explore similar analysis on strongly correlated large- N theories that lack well-defined quasiparticles. For example, studying OTOCs of the spin- S PXP model in semiclassical regime ($1 \ll S < \infty$) may reveal important insight into its stability. Additionally, investigating the stability and chaos of more conventional and

realistic models, such as the PXP model, is essential. While it might be challenging to study OTOCs and identify distinctive features in such models—due to the low dimensionality of their local Hilbert space, which often inhibits exponential growth of OTOCs even in chaotic systems [38]—considering scar states as vacua of the SM projector P_i (as defined in Eq. (2.1)) offers a promising approach.

Acknowledgments

I thank M. Müller for useful comments and thorough feedback on the manuscript. I am also indebted to C. Aron for stimulating discussions and teaching me the Keldysh path integral formalism through a doctoral course at EPFL. This work was supported by Grant No. 200020200558 of the SNSF.

A Derivation of the OTOC of the periodic orbit in the single-particle system

Here I provide a detailed derivation of the OTOC of QS [Eq. (3.13)] in the main text based on the Keldysh path integral approach. To construct the partition function I consider the following time evolution operator \tilde{U} ,

$$\tilde{U} = U(\infty, 0)U_0(0, -\infty), \quad (\text{A1})$$

where U and U_0 satisfy the following differential equation

$$i\hbar\frac{\partial}{\partial t}U(t, 0) = HU(t, 0), \quad i\hbar\frac{\partial}{\partial t}U_0(t, 0) = 0, \quad (\text{A2})$$

with the initial condition $U(0, 0) = U_0(0, 0) = 1$. Physically, \tilde{U} describes a sudden quench: until $t = 0$ the system does not evolve at all, and then from $t = 0$ the Hamiltonian H acts on the system. While adding U_0 seems a redundant procedure due to $U_0(t, 0) = U_0(0, t) = 1$, U_0 removes the boundary term in the path integral and for this reason one should keep it. The partition function is defined as

$$\begin{aligned} Z &= \langle g|\tilde{U}^\dagger\tilde{U}|g\rangle = \int D[a^*, a]e^{\frac{i}{\hbar}S_K} \\ S_K &= \int_{-\infty}^{\infty} dt \sum_{\gamma=\pm} \gamma L_\gamma \\ L_\gamma &= a_\gamma^*(t)i\frac{d}{dt}a_\gamma(t) - \theta(t)H[a_\gamma^*(t), a_\gamma(t)]. \end{aligned} \quad (\text{A3})$$

In order to consider the initial Gaussian wavepacket, the expectation value of the operator should be shifted, i.e., $\langle a_\gamma \rangle = \alpha_0(t = 0)$. This requires that the complex field in the action should also be shifted as $a_\gamma \mapsto \alpha_0 + a_\gamma$. Therefore the Lagrangian is re-written as

$$L_\gamma = a_\gamma^*(t)i\frac{d}{dt}a_\gamma(t) - \theta(t)H[\alpha_0^*(t) + a_\gamma^*(t), \alpha_0(t) + a_\gamma(t)]. \quad (\text{A4})$$

It is convenient to further rewrite the action in terms of the Keldysh basis a_c and a_q , which are defined as

$$a_c(t) = \frac{1}{\sqrt{2}}(a_+(t) + a_-(t)), \quad a_q(t) = \frac{1}{\sqrt{2}}(a_+(t) - a_-(t)). \quad (\text{A5})$$

The (quadratic) leading part of the Lagrangian L_{quad} becomes

$$\begin{aligned} L_{\text{quad}} = & a_c^*(t) \left(i \frac{d}{dt} - i0^+ \right) a_q(t) + a_q^*(t) \left(i \frac{d}{dt} + i0^+ \right) a_c(t) \\ & - \frac{\theta(t)}{2} \begin{pmatrix} a_c^*(t) & a_c(t) \end{pmatrix} M(t) \begin{pmatrix} a_q(t) \\ a_q^*(t) \end{pmatrix} - \frac{\theta(t)}{2} \begin{pmatrix} a_q^*(t) & a_q(t) \end{pmatrix} M(t) \begin{pmatrix} a_c(t) \\ a_c^*(t) \end{pmatrix}, \end{aligned} \quad (\text{A6})$$

where $M(t)$ is the monodromy matrix defined in Eq. (3.4). Note that perturbations arise both from (the higher-order derivatives of) H_0 and (the whole) H_n ($n \geq 1$). However, L_{quad} is sufficient to calculate the OTOC to the leading order in \hbar , as shown below.

The Green's functions \mathcal{G}^R , \mathcal{G}^A , and \mathcal{G}^K are defined as

$$\begin{aligned} i\mathcal{G}^R(t, t') &= \left\langle \begin{pmatrix} a_c(t) \\ a_c^*(t) \end{pmatrix} \begin{pmatrix} a_q^*(t') & a_q(t') \end{pmatrix} \right\rangle, \\ i\mathcal{G}^A(t, t') &= \left\langle \begin{pmatrix} a_q(t) \\ a_q^*(t) \end{pmatrix} \begin{pmatrix} a_c^*(t') & a_c(t') \end{pmatrix} \right\rangle, \\ i\mathcal{G}^K(t, t') &= \left\langle \begin{pmatrix} a_c(t) \\ a_c^*(t) \end{pmatrix} \begin{pmatrix} a_c^*(t') & a_c(t') \end{pmatrix} \right\rangle. \end{aligned} \quad (\text{A7})$$

From Eq. (A6) the bare retarded Green's function \mathcal{G}_0^R is

$$\mathcal{G}_0^R(t, t') = \hbar \left(\left(i \frac{d}{dt} + i0^+ \right) \sigma^3 - \theta(t) M(t) \right)^{-1} (t, t'), \quad (\text{A8})$$

where $\sigma^3 = \text{diag}(1, -1)$ is the Pauli matrix. The bare retarded Green's function G_0^R in the main text [Eq. (3.6)] is the (1, 1) component of \mathcal{G}^R . Eq. (A8) implies that the leading order of the OTOC [Eq. (3.7)] is \hbar^2 . Note that the same propagator can be obtained for $t, t' > 0$ even if one removes the step function, i.e.,

$$\mathcal{G}_0^R(t, t') = \hbar \left(\left(i \frac{d}{dt} + i0^+ \right) \sigma^3 - M(t) \right)^{-1} (t, t'), \quad (\text{A9})$$

for $t, t' > 0$. Indeed, Eq. (A8) and Eq. (A9) satisfy the same differential equation for $t, t' > 0$. Since $M(t)$ is periodic with period T ($M(t+T) = M(t)$), calculating Eq. (A9) amounts to a non-interacting Floquet problem, which one can be solved formally as

$$\mathcal{G}_0^R(t, t') = -i\hbar\theta(t-t') \sum_{\alpha} \psi_{\alpha}(t) \psi_{\alpha}^{\dagger}(t'). \quad (\text{A10})$$

$\psi_{\alpha}(t)$ is a Floquet normal mode with two components, satisfying

$$\left[\sigma^3 \left(i \frac{\partial}{\partial t} + i0^+ \right) - M(t) \right] \psi_{\alpha}(t) = 0. \quad (\text{A11})$$

Just like in Bloch's theorem, the normal mode is decomposed as a phase factor and a periodic function,

$$\psi_\alpha(t) = e^{\lambda_\alpha t} u_\alpha(t), \quad u_\alpha(t+T) = u_\alpha(t), \quad (\alpha = 1, 2). \quad (\text{A12})$$

This phase factor is a LE of the periodic orbit.

Finally, substituting Eq. (A10) into Eq. (3.7), the OTOC to the leading order is

$$C^{(0)}(t) = \hbar^2 \theta(t) \left| \sum_\alpha e^{\lambda_\alpha t} [u_\alpha(t) u_\alpha^\dagger(0)]_{11} \right|^2 \sim \hbar^2 e^{2\lambda t}, \quad (\text{A13})$$

where λ is the maximum among the real parts of the Lyapunov exponents, i.e., $\lambda = \max_\alpha (\text{Re } \lambda_\alpha)$.

Corrections to Eq (A13) can be systematically computed by standard perturbation theory. For the leading order in the OTOC, the only important perturbation is the fourth order derivatives of H_0 , i.e., ϕ^4 -like interactions. Such interactions can produce a Hartree diagram, which means that one has to solve a non-linear equation of motion for G^R . Thus such interactions might affect the LE even to the leading order. However, this correction is not important for the early time exponential growth of the OTOC. Furthermore, except for the Hartree term, one finds that perturbations only result in higher order corrections in \hbar by simple power-counting: corrections from H_n ($n \geq 1$) are trivially higher order since the corresponding part of the action $S_n = -\int dt H_n$ contains at least \hbar^0 in the prefactor while each propagator carries \hbar . The higher order derivatives of the monodromy matrix in H_0 also yield only higher order corrections. Indeed, at each perturbative expansion, the overall prefactor gives $1/\hbar$ while there are at least two propagators (\hbar^2) involved.

B Derivation of thermal properties

In this Appendix I study thermodynamic properties of the many-body model, and prove that the density of the b -boson [Eq. (4.8)] should be strictly positive in the large- N limit.

The action of the model is

$$S = \int_0^\beta d\tau \left[\sum_{k \in \text{BZ}} \sum_{\mu=1}^N a_{k\mu}^* (\partial_\tau + \xi_k) a_{k\mu} + b_{k\mu}^* (\partial_\tau + \xi_k) b_{k\mu} + J \sum_{i=1}^L \sum_{\mu=1}^N v_{ai} v_{bi} b_{i\mu}^* b_{i\mu} \right] \\ + \int_0^\beta d\tau N \sum_{i=1}^L \left[\frac{\Delta_{ai}}{2} \left(v_{ai} - \frac{1}{N} \sum_{\mu=1}^N (a_{i\mu} + a_{i\mu}^*)^2 \right) + \frac{\Delta_{bi}}{2} \left(v_{bi} - \frac{1}{N} \sum_{\mu=1}^N (b_{i\mu} + b_{i\mu}^*)^2 \right) \right], \quad (\text{B1})$$

where $\Delta_{a/bi}$ is a Lagrange multiplier. Assuming that $\Delta_{a/b}$ and $v_{a/b}$ is space-time independent, the action becomes

$$S|_{\Delta, v: \text{fixed}} = \frac{N}{2} \sum_{k \in \text{BZ}} \sum_{i\omega_n} \text{tr} \log \begin{pmatrix} -i\omega_n + \xi_k - \Delta_a & -\Delta_a \\ -\Delta_a & i\omega_n + \xi_{-k} - \Delta_a \end{pmatrix} \\ + \frac{N}{2} \sum_{k \in \text{BZ}} \sum_{i\omega_n} \text{tr} \log \begin{pmatrix} -i\omega_n + \xi_k + Jv_a v_b - \Delta_b & -\Delta_b \\ -\Delta_b & i\omega_n + \xi_{-k} + Jv_a v_b - \Delta_b \end{pmatrix} \\ + \frac{NL}{2T} (\Delta_a v_a + \Delta_b v_b), \quad (\text{B2})$$

where $\omega_n = 2\pi nT$ is the Matsubara frequency. The minimizing the action with respect to $\Delta_{a/b}$ and $v_{a/b}$ yields the mean-field equations,

$$\begin{aligned}
\Delta_a &= -\frac{Jv_b}{L} \sum_{k \in \text{BZ}} \frac{\xi_k + Jv_a v_b - \Delta_b}{E_{kb}} \coth\left(\frac{E_{kb}}{2T}\right) \\
\Delta_b &= -\frac{Jv_a}{L} \sum_{k \in \text{BZ}} \frac{\xi_k + Jv_a v_b - \Delta_b}{E_{kb}} \coth\left(\frac{E_{kb}}{2T}\right) \\
v_a &= \frac{1}{L} \sum_{k \in \text{BZ}} \frac{\xi_k}{E_{ka}} \coth\left(\frac{E_{ka}}{2T}\right) \\
v_b &= \frac{1}{L} \sum_{k \in \text{BZ}} \frac{\xi_k + Jv_a v_b}{E_{kb}} \coth\left(\frac{E_{kb}}{2T}\right),
\end{aligned} \tag{B3}$$

where the quasiparticle energy for the two bosonic modes, E_{ka} and E_{kb} , are defined as

$$\begin{aligned}
E_{ka} &= \sqrt{\xi_k(\xi_k - 2\Delta_a)} \\
E_{kb} &= \sqrt{(\xi_k + Jv_a v_b)(\xi_k + Jv_a v_b - 2\Delta_b)}.
\end{aligned} \tag{B4}$$

Multiplying the action Eq.(B2) by the temperature provides the free energy density. While the energy density can also be obtained by differentiating the action with respect to the temperature, one can instead explicitly evaluate the thermal average of the Hamiltonian with the mean-field action, which results in the following expression,

$$\begin{aligned}
\frac{F}{NL} &= \frac{1}{\beta L} \sum_{k \in \text{BZ}} \left[\log(e^{E_{ka}/2T} - e^{-E_{ka}/2T}) + \log(e^{E_{kb}/2T} - e^{-E_{kb}/2T}) \right] \\
&\quad + \frac{1}{2} (\Delta_a v_a + \Delta_b v_b) \\
\frac{E}{NL} &= \frac{1}{L} \sum_{k \in \text{BZ}} \frac{\xi_k(\xi_k - \Delta_a)}{2E_{ka}} \coth\left(\frac{E_{ka}}{2T}\right) \\
&\quad + \frac{1}{L} \sum_{k \in \text{BZ}} \left[\frac{(\xi_k + Jv_a v_b)(\xi_k + Jv_a v_b - \Delta_b)}{2E_{kb}} \coth\left(\frac{E_{kb}}{2T}\right) - \xi_k \right] - \frac{Jv_a v_b}{2},
\end{aligned} \tag{B5}$$

where T is the temperature.

Finally I will show that Eq.(B3) implies non-zero b -boson density [Eq.(4.8)] at any temperature by contradiction. The mean-field equation implies that the thermal expectation value of ρ_b satisfies the following relation,

$$\langle \rho_b \rangle = -\frac{\Delta_a}{2Jv_b} = -\frac{\Delta_b}{2Jv_a}. \tag{B6}$$

Suppose $\langle \rho_b \rangle = 0$. By Eq.(B6) it implies $\Delta_a = \Delta_b = 0$. The first two lines of Eq.(B3) implies

$$0 = -\frac{Jv_{a/b}}{L} \sum_{k \in \text{BZ}} \text{sgn}(\xi_k + Jv_a v_b) \coth\left(\frac{E_{kb}}{2}\right). \tag{B7}$$

This in turns implies that v_b should also be zero by the last line of Eq.(B3) because it reads

$$v_b = \frac{1}{L} \sum_{k \in \text{BZ}} \text{sgn}(\xi_k + Jv_a v_b) \coth\left(\frac{\beta E_{kb}}{2}\right), \tag{B8}$$

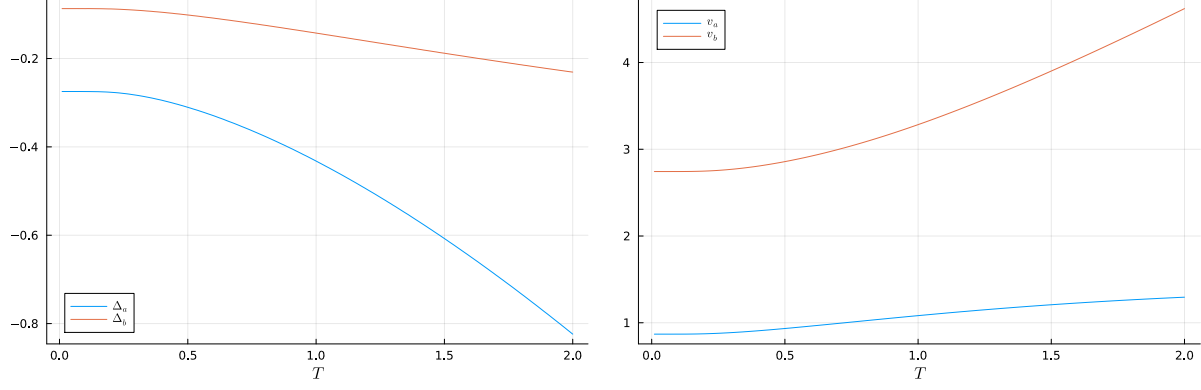


Figure 10: Solution of the mean-field equation Eq. (B3) as functions of the temperature T .

which indicates the relation $\Delta_a = -Jv_b^2 = 0$. However, if $v_b = 0$, the right-hand side of Eq. (B8) implies

$$0 = v_b = \frac{1}{L} \sum_{k \in \text{BZ}} \text{sgn}(\xi_k) \coth\left(\frac{\beta|\xi_k|}{2}\right) > 0, \quad (\text{B9})$$

which is a contradiction.

C Derivation of the Lyapunov exponent in QMBS

In this Appendix I provide a detailed derivation of the BS equation [Eq. (5.22)] in the main text based on the Keldysh path integral formalism. Following the main text I first derive the self-energy correction to the regarded Green's function in Sec. C.1, and then derive the BS equation in Sec. C.2.

The calculation below relies on the non-equilibrium Green's functions defined as,

$$\begin{aligned} iG^R(k; t, t') &= \theta(t - t') \langle \alpha | [b_{k\mu}(t), b_{k\mu}^\dagger(t')] | \alpha \rangle \\ iG^A(k; t, t') &= -\theta(t - t') \langle \alpha | [b_{k\mu}(t), b_{k\mu}^\dagger(t')] | \alpha \rangle \\ iG^K(k; t, t') &= \langle \alpha | \{b_{k\mu}(t), b_{k\mu}^\dagger(t')\} | \alpha \rangle. \end{aligned} \quad (\text{C1})$$

C.1 The regarded Green's function

The partition function of the system is written as

$$\begin{aligned} Z &= \langle \alpha | U^\dagger U | \alpha \rangle = \int D[a^*, a] D[b^*, b] e^{iS_K} \\ S_K &= \int_{-\infty}^{\infty} dt \sum_{\gamma=\pm} \gamma L_\gamma \\ L_\gamma &= \sum_{k \in \text{BZ}} \sum_{\mu=1}^N a_{k\mu\gamma}^*(t) i \frac{d}{dt} a_{k\mu\gamma}(t) + b_{k\mu\gamma}^*(t) i \frac{d}{dt} b_{k\mu\gamma}(t) - H_\gamma, \end{aligned} \quad (\text{C2})$$

where H_γ is the Hamiltonian with a_γ and b_γ fields. The equation of motion for those fields are

$$i \frac{da_{k\mu\gamma}}{dt} = \frac{\delta H_\gamma}{\delta a_{k\mu\gamma}^*(t)}, \quad i \frac{db_{k\mu\gamma}}{dt} = \frac{\delta H_\gamma}{\delta b_{k\mu\gamma}^*(t)}. \quad (\text{C3})$$

A solution of this equation is

$$a_{k\mu\gamma}(t) = \delta_{k,0} \alpha_\mu e^{-iEt}, \quad b_{k\mu\gamma}(t) = 0. \quad (\text{C4})$$

This solution corresponds to the perpetual oscillations of the initial scar state $|\alpha\rangle$. One can study the dynamics of the fluctuation by shifting a_γ field as $a_\gamma \mapsto a_\gamma + \alpha_\gamma$. I define the interacting term $L_{\text{int}} = \sum_{\gamma=\pm} \gamma L_{\text{int},\gamma}$ as follows,

$$\begin{aligned} L_{\text{int},\gamma} &= -\frac{J}{N^2} \sum_{i=1}^L \sum_{\mu\nu\rho=1}^N (4\alpha_\mu^2 \cos^2(Et) + 4\alpha_\mu \cos(Et)(a_{i\mu\gamma} + a_{i\mu\gamma}^*) + (a_{i\mu\gamma} + a_{i\mu\gamma}^*)^2) \\ &\quad \times (b_{i\nu\gamma} + b_{i\nu\gamma}^*)^2 b_{i\rho\gamma}^* b_{i\rho\gamma} \\ &\approx -\frac{4J\alpha^2}{N} \cos^2(Et) \sum_{i=1}^L \sum_{\mu\nu=1}^N b_{i\mu\gamma}^* b_{i\mu\gamma} (b_{i\nu\gamma} + b_{i\nu\gamma}^*)^2, \end{aligned} \quad (\text{C5})$$

where the approximation in the second line is valid under the assumption that $\alpha^2 = N^{-1} \sum_\mu \alpha_\mu^2$ is sufficiently large.

It is now convenient to rewrite L_{int} in the Keldysh basis (b_c and b_q),

$$\begin{aligned} L_{\text{int}} &\approx -\frac{2J\alpha^2}{N} \cos^2(Et) \sum_{i=1}^L \sum_{\mu\nu=1}^N (b_{i\mu c}^* b_{i\mu q} + b_{i\mu q}^* b_{i\mu c}) ((b_{i\nu c}^*)^2 + (b_{i\nu q}^*)^2 + b_{i\nu c}^2 + b_{i\nu q}^2) \\ &\quad - \frac{4J\alpha^2}{N} \cos^2(Et) \sum_{i=1}^L \sum_{\mu\nu=1}^N (b_{i\mu c}^* b_{i\mu q}^* + b_{i\mu c} b_{i\mu q}) (b_{i\nu c}^* b_{i\nu c} + b_{i\nu q}^* b_{i\nu q}) \\ &\quad - \frac{8J\alpha^2}{N} \cos^2(Et) \sum_{i=1}^L \sum_{\mu\nu=1}^N (b_{i\mu c}^* b_{i\mu q} + b_{i\mu q}^* b_{i\mu c}) (b_{i\nu c}^* b_{i\nu c} + b_{i\nu q}^* b_{i\nu q}). \end{aligned} \quad (\text{C6})$$

The retarded Green's function is then defined as $iG^R(t, t') = \langle b_c(t) b_q^*(t') \rangle$. As stated in the main text, the first order perturbation (the Hartree term) should vanish because the scar states are annihilated by $b_{i\mu}$. Up to the order of $1/N$, the second order perturbative correction to the retarded Green's function yields

$$-\int_{-\infty}^{\infty} dt_1 dt_2 G_0^R(k; t, t_1) \frac{8J^2\alpha^4}{N} \cos^2(Et_1) \cos^2(Et_2) \tilde{\Sigma}[G_0] G_0^R(k; t_2, 0), \quad (\text{C7})$$

where

$$\begin{aligned}
\tilde{\Sigma}[G_0] = & \frac{1}{L^2} \sum_{p,q \in \text{BZ}} G_0^R(p; t_1, t_2) G_0^R(q; t_1, t_2) G_0^R(k-p-q; t_1, t_2) \\
& + \frac{3}{L^2} \sum_{p,q \in \text{BZ}} G_0^R(p; t_1, t_2) G_0^K(q; t_1, t_2) G_0^K(k-p-q; t_1, t_2) \\
& + \frac{16}{L^2} \sum_{p,q \in \text{BZ}} G_0^R(p; t_1, t_2) G_0^K(q; t_1, t_2) G_0^K(-k+p+q; t_2, t_1) \\
& + \frac{2}{L^2} \sum_{p,q \in \text{BZ}} G_0^R(p; t_1, t_2) G_0^K(q; t_2, t_1) G_0^K(p-k-q; t_2, t_1) \\
& + \frac{8}{L^2} \sum_{p,q \in \text{BZ}} G_0^A(p; t_2, t_1) G_0^K(q; t_1, t_2) G_0^K(k+p-q; t_1, t_2) \\
& + \frac{6}{L^2} \sum_{p,q \in \text{BZ}} G_0^A(p; t_2, t_1) G_0^K(q; t_2, t_1) G_0^K(k+p+q; t_1, t_2).
\end{aligned} \tag{C8}$$

In the frequency space, the Dyson equation is written as,

$$G^R(k, \omega) = G_0^R(k, \omega) - G_0^R(k, \omega) \sum_{n \in \mathbb{Z}} \Sigma_n(k, \omega) G^R(k, \omega + 2nE), \tag{C9}$$

where

$$\begin{aligned}
\Sigma_0(k, \omega) &= -\frac{8J^2\alpha^4}{NL^2} \sum_{p,q \in \text{BZ}} \left(S^R(\omega, k, p, q) + \frac{1}{4} S^R(\omega + 2E, k, p, q) + \frac{1}{4} S^R(\omega - 2E, k, p, q) \right) \\
\Sigma_{\pm 1}(k, \omega) &= -\frac{4J^2\alpha^4}{NL^2} \sum_{p,q \in \text{BZ}} \left(S^R(\omega, k, p, q) + S^R(\omega \pm 2E, k, p, q) \right) \\
\Sigma_{\pm 2}(k, \omega) &= -\frac{2J^2\alpha^4}{NL^2} \sum_{p,q \in \text{BZ}} S^R(\omega \pm 2E, k, p, q) \\
\Sigma_{\pm n}(k, \omega) &= 0 \quad (n > 2).
\end{aligned} \tag{C10}$$

The factor S^R is defined as

$$\begin{aligned}
S^R(\omega, k, p, q) &= \frac{1}{\omega - \xi_p - \xi_q - \xi_{k-p-q} + i0^+} + \frac{2}{\omega + \xi_p - \xi_q - \xi_{k+p-q} + i0^+} \\
&\quad - \frac{1}{\omega + \xi_p + \xi_q - \xi_{k+p+q} + i0^+}.
\end{aligned} \tag{C11}$$

The imaginary part of the self-energy $\text{Im} \Sigma_n(k, \omega)$ is approximated by substituting

$$\begin{aligned}
S^R(\omega, k, p, q) \rightarrow & -\pi \left[\delta(\xi_k - \xi_p - \xi_q - \xi_{k-p-q}) + 2\delta(\xi_k + \xi_p - \xi_q - \xi_{k+p-q}) \right. \\
& \left. - \delta(\xi_k + \xi_p + \xi_q - \xi_{k+p+q} + i0^+) \right].
\end{aligned} \tag{C12}$$

into Eq. (C10). The first two terms in S^R represent the particle-number decreasing process and the number conserving process, respectively, and the last term is the number increasing process. Combined with Eq. (5.17) the approximate retarded Green's function is

$$G^R(k, \omega) \approx \frac{1}{\omega - \xi_k + \Sigma_k}, \tag{C13}$$

where

$$\begin{aligned}\Sigma_k &= -\frac{8J^2\alpha^4}{NL^2} \sum_{p,q \in \text{BZ}} \left(S^R(\xi_k, k, p, q) + \frac{1}{4}S^R(\xi_k + 2E, k, p, q) + \frac{1}{4}S^R(\xi_k - 2E, k, p, q) \right) \\ &\equiv \frac{8J^2\alpha^4}{N} \tilde{\Sigma}_k.\end{aligned}\tag{C14}$$

C.2 Bethe-Salpeter equation

In this section I will derive the BS equation in the main text [Eq. (5.22)], following equilibrium cases [32, 33]. Unlike the Green's function, one needs to double the degrees of freedom to regard the OTOC as a path-ordered correlator. The partition function with the two folded Keldysh contour is,

$$\begin{aligned}Z &= \int D[a^*, a]D[b^*, b]e^{iS_K} \\ S_K &= \sum_{p=u,d} \sum_{\gamma=\pm} \gamma S_{p\gamma} \\ S_{p\gamma} &= \int_{-\infty}^{\infty} dt \sum_{k \in \text{BZ}} \sum_{\mu=1}^N \left[a_{k\mu p\gamma}^*(t) i \frac{d}{dt} a_{k\mu p\gamma}(t) + b_{k\mu p\gamma}^*(t) i \frac{d}{dt} b_{k\mu p\gamma}(t) \right] - H_{p\gamma}.\end{aligned}\tag{C15}$$

To carry out perturbative calculations I follow the idea of sudden quench in the single-particle case: since one only needs to consider the system for the period $0 \leq \tau \leq t$, it is sufficient to introduce the interaction term in the action for this period, i.e., S_{int} is defined as

$$S_{\text{int}} = \int_0^t d\tau L_{\text{int}}.\tag{C16}$$

This way of introducing the interaction does not affect the final result, and simplifies calculations since one can take advantage of the causality (any field $\phi(\tau)$ in S_{int} should satisfy $0 \leq \tau \leq t$).

In order to derive the BS equation for the OTOC, I consider the Laplace transform of $C_\alpha(t)$ as

$$\begin{aligned}C_\alpha(\omega) &= \int_0^\infty dt e^{i\omega t} C_\alpha(t) \\ C_\alpha(t) &= \int \frac{d\omega}{2\pi} e^{-i\omega t} C_\alpha(\omega),\end{aligned}\tag{C17}$$

where for the inverse transformation the integral contour should run above all the singularities. Note that the conventional Fourier transformation is insufficient since the exponential function cannot be Fourier transformed. In the following I will compute $C_\alpha(\omega)$ perturbatively, and derive the BS equation for the OTOC.

C.2.1 The zeroth order

The zeroth order of the OTOC is already presented in the main text [Eq. (5.10)]. Its Laplace transform is

$$C_\alpha^{(0)}(\omega) = \frac{1}{NL} \int \frac{dk_0}{2\pi} \sum_{k \in \text{BZ}} G_0^R(k, k_0) (G_0^R(k, k_0 - \omega))^* \equiv \frac{1}{NL} \int \frac{dk_0}{2\pi} \sum_{k \in \text{BZ}} f^{(0)}(k, k_0, \omega),\tag{C18}$$

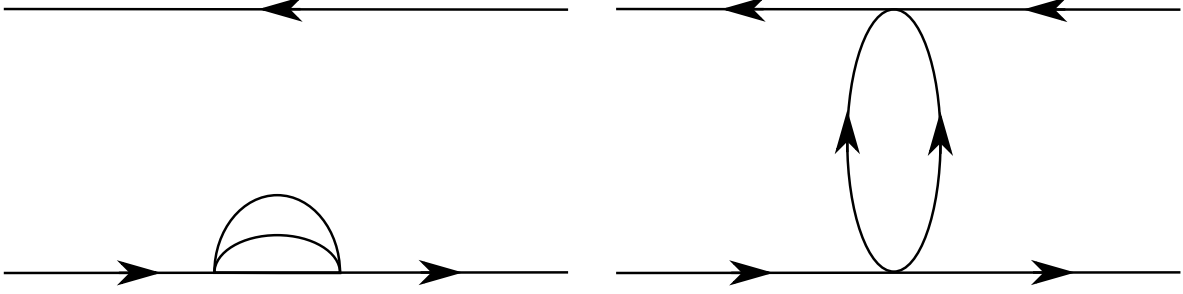


Figure 11: Typical diagrams of the second order corrections to the OTOC. They include (i) the correction to the propagator (the left panel) and (ii) the one peculiar to the OTOC (the right panel).

where k_0 runs above all the singularities too. When higher order corrections are considered in Sec. C.2.4, Eq. (C18) should be replaced with the full propagators. However, such a term is irrelevant for the Lyapunov growth of the OTOC, since Σ_k [Eq. (C14)] is positive, which implies that Eq. (C18) has a pole in the lower half plane and thus $C_\alpha^{(0)}(t)$ decays in time.

C.2.2 The first order

As stated in the main text in Sec. 5.1.1 (or Sec. C.1), the first order perturbation should vanish, as any normal ordered operator should annihilate the scar states.

C.2.3 The second order

The second order perturbations are classified as (i) perturbations to the Green's function (the left panel of Fig. 11) and (ii) a perturbation peculiar to the OTOC (the right panel of Fig. 11). The perturbations (i) have been already discussed in Sec. C.1, so I focus on the perturbation (ii). Unlike the correction to the Green's function that contains many terms [Eq. (C8)], the perturbation (ii) consists of only one term,

$$\int_0^t dt_1 dt_2 \frac{1}{NL} \sum_{k \in \text{BZ}} G_0^R(k; t, t_1) (G_0^R(k; t, t_2))^* \frac{8J^2 \alpha^4}{NL^2} \cos^2(Et_1) \cos^2(Et_2) \times \sum_{p, q \in \text{BZ}} G_0^W(p; t_1, t_2) G_0^W(k - p - q; t_1, t_2) G_0^R(q; t_1, 0) (G_0^R(q; t_2, 0))^*, \quad (\text{C19})$$

where G_0^W is the zeroth order approximation of (an analog of) the Wightman function $G^W(t, t') = \langle \alpha | b(t) b^\dagger(t') | \alpha \rangle$. As shown in Fig. 11, the second order correction to the OTOC corresponds to adding a “rung diagram” to the set of the bare propagators. The domain of the integral can now be extended from $[0, t]$ to $[-\infty, \infty]$ due to the causality structure of the retarded Green's function ($G^R(t, t') \propto \theta(t - t')$).

In the frequency space, the above equation is written as,

$$\int \frac{dk_0 dq_0}{(2\pi)^2} \frac{1}{NL} \sum_{k \in \text{BZ}} f^{(0)}(k, k_0, \omega) \sum_{n \in \mathbb{Z}} \sum_{q \in \text{BZ}} R_n(k, k_0; q, q_0) f^{(0)}(q, q_0, \omega + 2nE), \quad (\text{C20})$$

where R_n is defined as

$$\begin{aligned}
R_0(k, k_0; q, q_0) &= \frac{2J^2\alpha^4}{NL^2} \sum_{p \in \text{BZ}} G_0^W(k-p-q, k_0-q_0-\xi_p) \\
&\quad + \frac{J^2\alpha^4}{2NL^2} \sum_{p \in \text{BZ}} G_0^W(k-p-q, k_0-q_0-\xi_p+2E) \\
&\quad + \frac{J^2\alpha^4}{2NL^2} \sum_{p \in \text{BZ}} G_0^W(k-p-q, k_0-q_0-\xi_p-2E) \\
R_{\pm 1}(k, k_0; q, q_0) &= \frac{J^2\alpha^4}{NL^2} \sum_{p \in \text{BZ}} G_0^W(k-p-q, k_0-q_0-\xi_p) \\
&\quad + \frac{J^2\alpha^4}{NL^2} \sum_{p \in \text{BZ}} G_0^W(k-p-q, k_0-q_0-\xi_p \pm 2E) \\
R_{\pm 2}(k, k_0; q, q_0) &= \frac{J^2\alpha^4}{2NL^2} \sum_{p \in \text{BZ}} G_0^W(k-p-q, k_0-q_0-\xi_p \pm 2E) \\
R_{\pm n}(k, k_0; q, q_0) &= 0 \quad (n > 2).
\end{aligned} \tag{C21}$$

C.2.4 Higher order

The above exercise (Eq. (C18) and Eq. (C20)) implies that the higher order perturbations correspond to adding many rung diagrams and thus they can be incorporated by replacing the bare correlator with the full correlator: let us write the OTOC in the momentum space as

$$C_\alpha(\omega) = \int \frac{dk_0}{2\pi} \frac{1}{NL} \sum_{k \in \text{BZ}} f(k, k_0, \omega). \tag{C22}$$

At the zeroth order in J , $f(k, k_0, \omega) = f^{(0)}(k, k_0, \omega) + O(J)$. The effect of higher order corrections is modifying the Green's function and adding the rung diagram. Therefore, $f(k, k_0, \omega)$ satisfies the following BS equation,

$$\begin{aligned}
f(k, k_0, \omega) &= G^R(k, k_0)(G^R(k, k_0 - \omega))^* \\
&\quad + G^R(k, k_0)(G^R(k, k_0 - \omega))^* \int \frac{dq_0}{2\pi} \sum_{n \in \mathbb{Z}} \sum_{q \in \text{BZ}} R(k, k_0; q, q_0) f(q, q_0, \omega + 2nE).
\end{aligned} \tag{C23}$$

As mentioned in Sec. C.2.1, one can safely neglect the first term in the RHS for the asymptotic rate of the Lyapunov growth since it describes decay of the quasiparticles. I further approximate Eq. (C23) by imposing the on-shell condition,

$$G^R(k, k_0)(G^R(k, k_0 - \omega))^* \approx i\pi \frac{\delta(k_0 - \xi_k)}{\omega + i \text{Im} \Sigma_k}, \tag{C24}$$

which is an analog of the quasiparticle approximation in the derivation of the Boltzmann equation. Substituting Eq. (C24) into Eq. (C23), one arrives at the BS equation,

$$-i\omega f(k, \omega) \approx -\text{Im} \Sigma_k f(k, \omega) + \sum_{n \in \mathbb{Z}} \sum_{q \in \text{BZ}} K_{-n}(k, q) f(q, \omega + 2nE), \tag{C25}$$

where $f(k, \omega) = f(k, \xi_k, \omega)$ and the kernel K is defined as $K_{-n}(k, q) = R_n(k, \xi_k, q, \xi_q)/2$.

To solve this equation, I define the “vector”

$$f_n(k, \omega) = f(k, \omega + 2nE), \quad (\text{C26})$$

and with this notation Eq. (C25) is written as the Schrödinger equation of periodically driven systems,

$$-i(\omega + 2nE)f_n(k, \omega) \approx -\text{Im} \Sigma_k f_n(k, \omega) + \sum_{m \in \mathbb{Z}} \sum_{q \in \text{BZ}} K_{-m}(k, q) f_{n+m}(q, \omega). \quad (\text{C27})$$

I regard $-\text{Im} \Sigma_k$ and $K_{-m}(k, q)$ as a Fourier series of the periodic (matrix) function $\hat{K}(t)$,

$$\langle k | \hat{K}(t) | q \rangle \equiv -\delta_{k,q} \text{Im} \Sigma_k + K(k, q, t) = \sum_{n \in \mathbb{Z}} e^{-i2nEt} (-\text{Im} \Sigma_k \delta_{k,q} \delta_{n,0} + K_n(k, q)). \quad (\text{C28})$$

Eq. (C27) is then equivalent to the Schrödinger equation $\frac{d}{dt} |f(t)\rangle = \hat{K}(t) |f(t)\rangle$. The Schrödinger equation is formally solved by exponentiating the kernel $\hat{K}(t)$, which is expanded as the Magnus series,

$$|f(t)\rangle = \mathcal{T} \exp \left[\int_0^t d\tau \hat{K}(\tau) \right] |f\rangle, \quad \mathcal{T} \exp \left[\int_0^t d\tau \hat{K}(\tau) \right] = \exp \left[\hat{\Omega}_K(t) \right], \quad (\text{C29})$$

where \mathcal{T} is the time-ordered product and

$$\begin{aligned} \hat{\Omega}_K(t) &= \sum_{n=1}^{\infty} \hat{\Omega}_n(t) \\ \hat{\Omega}_1(t) &= \int_0^t d\tau \hat{K}(\tau) \\ \hat{\Omega}_2(t) &= \int_0^t d\tau_1 \int_0^{\tau_1} d\tau_2 [\hat{K}(\tau_1), \hat{K}(\tau_2)] \\ &\vdots \end{aligned} \quad (\text{C30})$$

$\hat{\Omega}_1$ is already sufficient for the Lyapunov exponent to be correctly calculated up to the order of $1/N$, as each matrix element of $\hat{K}(t)$ is of order $1/N$. If one sets $t = n\pi/E$, $\hat{\Omega}_1$ corresponds to K_0 . Therefore, Eq. (5.23) is justified.

D Derivation of the OTOC of another unstable periodic orbit

In this Appendix I aim to derive the OTOC of the periodic orbit $|\beta\rangle$ [Eq. (6.1)], following closely the derivation of the OTOCs in the previous cases.

The unstable periodic orbit Eq. (6.1) corresponds to the following solution of the equation of motion of the Keldysh action [Eq. (C3)],

$$a_{k\mu\gamma}(t) = 0, \quad b_{k\mu\gamma}(t) = \delta_{k,0} \beta_\mu e^{-iEt}. \quad (\text{D1})$$

Following the idea of the sudden quench in Appendix A, the interacting term $L_{\text{int}} = \sum_{\gamma=\pm} \gamma L_{\text{int},\gamma}$ is written as,

$$L_{\text{int},\gamma} = -\frac{J\theta(t)}{N^2} \sum_{i=1}^L \sum_{\mu\nu\rho=1}^N (\beta_\mu^* e^{iEt} + b_{i\mu\gamma}) (\beta_\mu e^{-iEt} + b_{i\mu\gamma}) (a_{i\nu\gamma} + a_{i\nu\gamma}^*)^2. \quad (\text{D2})$$

Assuming $\beta^2 := N^{-1} \sum_\mu |\beta_\mu|^2$ is sufficiently large, the dominant term in L_{int} is

$$\begin{aligned} L_{\text{int}} &\approx -8J\theta(t)\beta^2 \cos^2(Et) \sum_{i=1}^L \sum_{\mu=1}^N (a_{i\mu c} + a_{i\mu c}^*) (a_{i\mu q} + a_{i\mu q}^*) \\ &\equiv -2\mathcal{J}(t) \sum_{i=1}^L \sum_{\mu=1}^N (a_{i\mu c} + a_{i\mu c}^*) (a_{i\mu q} + a_{i\mu q}^*). \end{aligned} \quad (\text{D3})$$

Note that unlike the initial scar state in Appendix C, the dominant term is quadratic, which implies that L_{int} affects the OTOC even at the leading order. Indeed, the quadratic part of the full Lagrangian L_{quad} is

$$\begin{aligned} L_{\text{quad}} &= \frac{1}{2} \sum_{k \in \text{BZ}} \sum_{\mu=1}^N (a_{k\mu c}^* \quad a_{-k\mu c}) \begin{pmatrix} i\partial_t - i0 - \xi_k - \mathcal{J}(t) & \mathcal{J}(t) \\ -\mathcal{J}(t) & -i\partial_t + i0 - \xi_{-k} - \mathcal{J}(t) \end{pmatrix} \begin{pmatrix} a_{k\mu q} \\ a_{-k\mu q}^* \end{pmatrix} \\ &+ \frac{1}{2} \sum_{k \in \text{BZ}} \sum_{\mu=1}^N (a_{k\mu q}^* \quad a_{-k\mu q}) \begin{pmatrix} i\partial_t + i0 - \xi_k - \mathcal{J}(t) & \mathcal{J}(t) \\ -\mathcal{J}(t) & -i\partial_t - i0 - \xi_{-k} - \mathcal{J}(t) \end{pmatrix} \begin{pmatrix} a_{k\mu c} \\ a_{-k\mu c}^* \end{pmatrix} \\ &+ 2i0 \sum_{k \in \text{BZ}} a_{k\mu q}^* a_{k\mu q}. \end{aligned} \quad (\text{D4})$$

Following Appendix A, I define the Green's function as,

$$\begin{aligned} i\mathcal{G}^R(k; t, t') &= \left\langle \left\langle \begin{pmatrix} a_{k\mu c}(t) \\ a_{-k\mu c}^*(t) \end{pmatrix} \begin{pmatrix} a_{k\mu q}(t') & a_{-k\mu q}^*(t') \end{pmatrix} \right\rangle \right\rangle \\ i\mathcal{G}^A(k; t, t') &= \left\langle \left\langle \begin{pmatrix} a_{k\mu q}(t) \\ a_{-k\mu q}^*(t) \end{pmatrix} \begin{pmatrix} a_{k\mu c}(t') & a_{-k\mu c}^*(t') \end{pmatrix} \right\rangle \right\rangle \\ i\mathcal{G}^K(k; t, t') &= \left\langle \left\langle \begin{pmatrix} a_{k\mu c}(t) \\ a_{-k\mu c}^*(t) \end{pmatrix} \begin{pmatrix} a_{k\mu c}(t') & a_{-k\mu c}^*(t') \end{pmatrix} \right\rangle \right\rangle. \end{aligned} \quad (\text{D5})$$

The retarded Green's function defined in the main text (Eq. (6.4)) is the (1,1)-component of \mathcal{G}^R .

At the leading order, \mathcal{G}^R is easily obtained,

$$\mathcal{G}^R(k; t, t') = -i\theta(t) \sum_{\alpha} \psi_{k\alpha}(t) \psi_{k\alpha}^\dagger(t'), \quad t, t' > 0, \quad (\text{D6})$$

where $\psi_{k\alpha}$ is the Floquet normal mode satisfying

$$\left[\sigma^3 \left(i \frac{d}{dt} + i0^+ \right) - \begin{pmatrix} \xi_k + \mathcal{J}(t) & \mathcal{J}(t) \\ \mathcal{J}(t) & \xi_{-k} + \mathcal{J}(t) \end{pmatrix} \right] \psi_{k\alpha}(t) = 0. \quad (\text{D7})$$

Again, the Floquet normal mode $\psi_{k\alpha}$ satisfies the relation

$$\psi_{k\alpha}(t) = e^{\lambda_{k\alpha} t} u_{k\alpha}(t), \quad u_{k\alpha}(t + \pi/E) = u_{k\alpha}(t). \quad (\text{D8})$$

Therefore, the exponential factor in the normal mode corresponds to the Lyapunov exponent and the OTOC at the leading order is expressed as,

$$C_\beta(t) = \frac{\theta(t)}{NL} \sum_{k \in \text{BZ}} \left| \sum_{\alpha} e^{\lambda_{k\alpha} t} [u_{k\alpha}(t) u_{k\alpha}^\dagger(0)]_{11} \right|^2. \quad (\text{D9})$$

E Derivation of the OTOC with the scar-breaking perturbation

In this section I will derive the OTOC of the periodic orbit when the scar-breaking term V is added. To this end, I define the following Green's function,

$$\mathcal{G}(k; t, t') = \begin{pmatrix} \mathcal{G}^K(k; t, t') & \mathcal{G}^R(k; t, t') \\ \mathcal{G}^A(k; t, t') & 0 \end{pmatrix}, \quad (\text{D10})$$

where each component is defined as,

$$\begin{aligned} i\mathcal{G}^R(k; t, t') &= \left\langle \left(\begin{array}{c} b_{k\mu c}(t) \\ b_{-k\mu c}^*(t) \end{array} \right) \left(\begin{array}{cc} b_{k\mu q}^*(t') & b_{-k\mu q}(t') \end{array} \right) \right\rangle \\ i\mathcal{G}^A(k; t, t') &= \left\langle \left(\begin{array}{c} b_{k\mu q}(t) \\ b_{-k\mu q}^*(t) \end{array} \right) \left(\begin{array}{cc} b_{k\mu c}^*(t') & b_{-k\mu c}(t') \end{array} \right) \right\rangle \\ i\mathcal{G}^K(k; t, t') &= \left\langle \left(\begin{array}{c} b_{k\mu c}(t) \\ b_{-k\mu c}^*(t) \end{array} \right) \left(\begin{array}{cc} b_{k\mu c}^*(t') & b_{-k\mu c}(t') \end{array} \right) \right\rangle. \end{aligned} \quad (\text{D11})$$

In the following I denote τ^a and σ^a as the Pauli matrices acting on the Keldysh space and the particle-hole space, respectively.

Note that the quadratic part of the Lagrangian is modified by the perturbation,

$$\begin{aligned} L_{\text{quad}} &= \sum_{k \in \text{BZ}} \sum_{\mu=1}^N (a_{k\mu c}^* \ a_{k\mu q}) \begin{pmatrix} 0 & i\partial_t - i0 - \xi_k \\ i\partial_t + i0 - \xi_k & 2i0 \end{pmatrix} \begin{pmatrix} a_{k\mu c} \\ a_{k\mu q} \end{pmatrix} \\ &+ \frac{1}{2} \sum_{k \in \text{BZ}} \sum_{\mu=1}^N (b_{k\mu c}^* \ b_{-k\mu c}) \begin{pmatrix} i\partial_t - i0 - \xi_k & \theta(t)\epsilon \\ \theta(t)\epsilon & -i\partial_t + i0 - \xi_k \end{pmatrix} \begin{pmatrix} b_{k\mu q} \\ b_{-k\mu q}^* \end{pmatrix} \\ &+ \frac{1}{2} \sum_{k \in \text{BZ}} \sum_{\mu=1}^N (b_{k\mu q}^* \ b_{-k\mu q}) \begin{pmatrix} i\partial_t + i0 - \xi_k & \theta(t)\epsilon \\ \theta(t)\epsilon & -i\partial_t - i0 - \xi_k \end{pmatrix} \begin{pmatrix} b_{k\mu q} \\ b_{-k\mu q}^* \end{pmatrix} \\ &+ 2i0 \sum_{k \in \text{BZ}} \sum_{\mu=1}^N b_{k\mu q}^* b_{k\mu q}. \end{aligned} \quad (\text{D12})$$

As one can see the discussion below, L_{quad} might already indicate the chaos of the periodic orbit when the perturbation is strong enough, while for the weak perturbation one has to check the higher orders to detect the chaotic dynamics of the OTOC.

E.1 The case $|\epsilon| > E$

When the perturbation satisfies the condition $|\epsilon| > E$, the OTOC exhibits the exponential growth just as QS (Appendix. A) and the unstable periodic orbit (Appendix. D).

For $t, t' > 0$, the retarded Green's function shows different behaviors depending on the sign of $\xi_k^2 - \epsilon^2$. If $\xi_k^2 > \epsilon^2$, it is

$$\begin{aligned} i\mathcal{G}^R(k; t, t') = & \theta(t-t') \frac{e^{-i\sqrt{\xi_k^2 - \epsilon^2}t}}{2\sqrt{\xi_k^2 - \epsilon^2}} \begin{pmatrix} \sqrt{\xi_k^2 - \epsilon^2} + \xi_k & \epsilon \\ \epsilon & -\sqrt{\xi_k^2 - \epsilon^2} + \xi_k \end{pmatrix} \\ & - \theta(t-t') \frac{e^{i\sqrt{\xi_k^2 - \epsilon^2}t}}{2\sqrt{\xi_k^2 - \epsilon^2}} \begin{pmatrix} -\sqrt{\xi_k^2 - \epsilon^2} + \xi_k & \epsilon \\ \epsilon & \sqrt{\xi_k^2 - \epsilon^2} + \xi_k \end{pmatrix}. \end{aligned} \quad (\text{D13})$$

If $\xi_k^2 < \epsilon^2$, it shows the exponential growth,

$$\begin{aligned} i\mathcal{G}^R(k; t, t') = & \frac{e^{\sqrt{\epsilon^2 - \xi_k^2}t}}{2i\sqrt{\epsilon^2 - \xi_k^2}} \begin{pmatrix} i\sqrt{\epsilon^2 - \xi_k^2} + \xi_k & \epsilon \\ \epsilon & -i\sqrt{\epsilon^2 - \xi_k^2} + \xi_k \end{pmatrix} \\ & - \frac{e^{-\sqrt{\epsilon^2 - \xi_k^2}t}}{2i\sqrt{\epsilon^2 - \xi_k^2}} \begin{pmatrix} -i\sqrt{\epsilon^2 - \xi_k^2} + \xi_k & \epsilon \\ \epsilon & i\sqrt{\epsilon^2 - \xi_k^2} + \xi_k \end{pmatrix}. \end{aligned} \quad (\text{D14})$$

Therefore, to the leading order the OTOC shows the exponential growth.

E.2 The case $|\epsilon| < E$

Eq. (D13) indicates that the quadratic term of the Lagrangian is not enough to obtain the chaos when the perturbation satisfies $|\epsilon| < E$, which requires that one should treat the interaction. For the interacting term L_{int} [Eq. (C5)], only the first-order correction (Fig. 3) survives in the large- N limit,

$$\begin{aligned} \mathcal{G}(k; t, t') = & \mathcal{G}_0(k; t, t') + \int d\tau \Sigma(\tau) \mathcal{G}_0(k; t, \tau) \tau^1 \mathcal{G}(k; \tau, t') \\ & + \int d\tau \Sigma'(\tau) \mathcal{G}_0(k; t, \tau) \tau^1 \otimes \sigma^1 \mathcal{G}(k; \tau, t'), \end{aligned} \quad (\text{D15})$$

where the self-energies Σ and Σ' are defined as

$$\begin{aligned} \Sigma(\tau) = & \frac{8J\alpha^2}{L} \sum_{q \in \text{BZ}} \sinh(2\theta_q) (2\sinh(2\theta_q) + \cosh(2\theta_q)) \cos^2(E\tau) \sin^2(\sqrt{\xi_q^2 - \epsilon^2}\tau) \\ \Sigma'(\tau) = & \frac{8J\alpha^2}{L} \sum_{q \in \text{BZ}} \sinh^2(2\theta_q) \cos^2(E\tau) \sin^2(\sqrt{\xi_q^2 - \epsilon^2}\tau), \end{aligned} \quad (\text{D16})$$

with

$$\theta_q = \text{arctanh} \left(\frac{\xi_q - \sqrt{\xi_q^2 - \epsilon^2}}{\epsilon} \right). \quad (\text{D17})$$

Note that in order to find the early time growth of the OTOC, this treatment is enough, while for later time one needs to solve the Hartree equation, i.e., the self-energy should be a functional of the full Green's function.

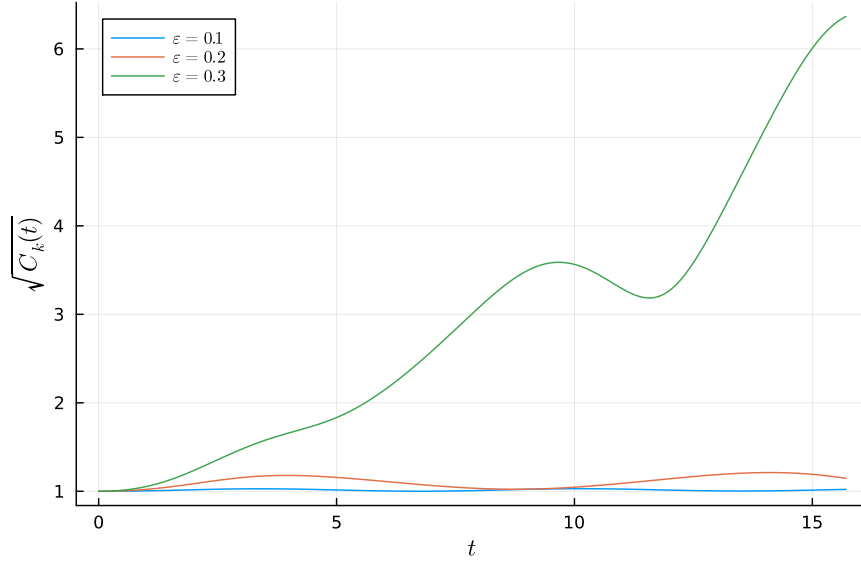


Figure 12: The OTOC $C_k(t)$ at $k = 0$ for $\xi_k = -2 \cos k + 2.5$, $8J\alpha^2 = 3$.

The Dyson equation [Eq. (D15)] indicates that the retarded Green's function should satisfy the following Dyson equation,

$$\mathcal{G}^R(k; t, 0) = \mathcal{G}_0^R(k; t, 0) + \int_0^t d\tau \mathcal{G}_0^R(k; t, \tau) (\Sigma(\tau) + \Sigma'(\tau)\sigma^1) \mathcal{G}^R(k; \tau, 0). \quad (\text{D18})$$

This equation is solved numerically iteratively by updating the Green's function by the equation,

$$\mathcal{G}_{n+1}^R(k; t, 0) = \mathcal{G}_0^R(k; t, 0) + \int_0^t d\tau \mathcal{G}_0^R(k; t, \tau) (\Sigma(\tau) + \Sigma'(\tau)\sigma^1) \mathcal{G}_n^R(k; \tau, 0), \quad (\text{D19})$$

until the algorithm converges.

Note that the OTOC is approximately expanded as,

$$C_\alpha(t) = \frac{\theta(t)}{N} \sum_{k \in \text{BZ}} C_k(t). \quad (\text{D20})$$

To the leading order $C_k(t)$ is a product of the retarded Green's function. I observe numerically that the modes around $k = 0$ show the most significant chaotic behavior. Furthermore, $C_{k=0}$ in Fig. 12 shows that for the small ϵ the growth of the OTOC is extremely slow.

References

- [1] J. M. Deutsch. Quantum statistical mechanics in a closed system. *Phys. Rev. A*, 43:2046–2049, Feb 1991.
- [2] Mark Srednicki. Chaos and quantum thermalization. *Phys. Rev. E*, 50:888–901, Aug 1994.

- [3] Marcos Rigol, Vanja Dunjko, and Maxim Olshanii. Thermalization and its mechanism for generic isolated quantum systems. *Nature*, 452(7189):854–858, Apr 2008.
- [4] Naoto Shiraishi and Takashi Mori. Systematic construction of counterexamples to the eigenstate thermalization hypothesis. *Phys. Rev. Lett.*, 119:030601, Jul 2017.
- [5] Takashi Mori and Naoto Shiraishi. Thermalization without eigenstate thermalization hypothesis after a quantum quench. *Phys. Rev. E*, 96:022153, Aug 2017.
- [6] Hannes Bernien, Sylvain Schwartz, Alexander Keesling, Harry Levine, Ahmed Omran, Hannes Pichler, Soonwon Choi, Alexander S. Zibrov, Manuel Endres, Markus Greiner, Vladan Vuletić, and Mikhail D. Lukin. Probing many-body dynamics on a 51-atom quantum simulator. *Nature*, 551(7682):579–584, Nov 2017.
- [7] C. J. Turner, A. A. Michailidis, D. A. Abanin, M. Serbyn, and Z. Papić. Weak ergodicity breaking from quantum many-body scars. *Nature Physics*, 14(7):745–749, Jul 2018.
- [8] Eric J. Heller. Bound-state eigenfunctions of classically chaotic hamiltonian systems: Scars of periodic orbits. *Phys. Rev. Lett.*, 53:1515–1518, Oct 1984.
- [9] Sanjay Moudgalya, Stephan Rachel, B. Andrei Bernevig, and Nicolas Regnault. Exact excited states of nonintegrable models. *Phys. Rev. B*, 98:235155, Dec 2018.
- [10] Michael Schechter and Thomas Iadecola. Weak ergodicity breaking and quantum many-body scars in spin-1 xy magnets. *Phys. Rev. Lett.*, 123:147201, Oct 2019.
- [11] Thomas Iadecola and Michael Schechter. Quantum many-body scar states with emergent kinetic constraints and finite-entanglement revivals. *Phys. Rev. B*, 101:024306, Jan 2020.
- [12] Daniel K. Mark, Cheng-Ju Lin, and Olexei I. Motrunich. Unified structure for exact towers of scar states in the affleck-kennedy-lieb-tasaki and other models. *Phys. Rev. B*, 101:195131, May 2020.
- [13] Sanjay Moudgalya and Olexei I. Motrunich. Exhaustive characterization of quantum many-body scars using commutant algebras, 2023.
- [14] Keita Omiya and Markus Müller. Quantum many-body scars in bipartite rydberg arrays originating from hidden projector embedding. *Phys. Rev. A*, 107:023318, Feb 2023.
- [15] Keita Omiya and Markus Müller. Fractionalization paves the way to local projector embeddings of quantum many-body scars. *Phys. Rev. B*, 108:054412, Aug 2023.
- [16] Wen Wei Ho, Soonwon Choi, Hannes Pichler, and Mikhail D. Lukin. Periodic orbits, entanglement, and quantum many-body scars in constrained models: Matrix product state approach. *Phys. Rev. Lett.*, 122:040603, Jan 2019.
- [17] Quirin Hummel, Klaus Richter, and Peter Schlagheck. Genuine Many-Body Quantum Scars along Unstable Modes in Bose-Hubbard Systems. *Phys. Rev. Lett.*, 130:250402, Jun 2023.

- [18] Bertrand Evrard, Andrea Pizzi, Simeon I. Mistakidis, and Ceren B. Dag. Quantum Scars and Regular Eigenstates in a Chaotic Spinor Condensate. *Phys. Rev. Lett.*, 132:020401, Jan 2024.
- [19] Markus Müller and Ruslan Mushkaev. Semiclassical origin of suppressed quantum chaos in rydberg chains, 2024.
- [20] Anatoly I. Larkin and Yu. N. Ovchinnikov. Quasiclassical method in the theory of superconductivity. *Journal of Experimental and Theoretical Physics*, 1969.
- [21] Ignacio García-Mata, Rodolfo Jalabert, and Diego Wisniacki. Out-of-time-order correlations and quantum chaos. *Scholarpedia*, 18(4):55237, 2023.
- [22] Vedika Khemani, Chris R. Laumann, and Anushya Chandran. Signatures of integrability in the dynamics of rydberg-blockaded chains. *Physical Review B*, 99(16), April 2019.
- [23] Cheng-Ju Lin, Anushya Chandran, and Olexei I. Motrunich. Slow thermalization of exact quantum many-body scar states under perturbations. *Phys. Rev. Research*, 2:033044, Jul 2020.
- [24] Patrice Kolb and Kiryl Pakrouski. Stability of the Many-Body Scars in Fermionic Spin-1/2 Models. *PRX Quantum*, 4(4), December 2023.
- [25] Alessio Lerose, Tommaso Parolini, Rosario Fazio, Dmitry A. Abanin, and Silvia Pappalardi. Theory of robust quantum many-body scars in long-range interacting systems, 2023.
- [26] Sanjay Moudgalya, Nicolas Regnault, and B. Andrei Bernevig. η -pairing in hubbard models: From spectrum generating algebras to quantum many-body scars. *Phys. Rev. B*, 102:085140, Aug 2020.
- [27] Anushya Chandran, Thomas Iadecola, Vedika Khemani, and Roderich Moessner. Quantum Many-Body Scars: A Quasiparticle Perspective. *Annual Review of Condensed Matter Physics*, 14(Volume 14, 2023):443–469, 2023.
- [28] Stephen H. Shenker and Douglas Stanford. Black holes and the butterfly effect. *Journal of High Energy Physics*, 2014(3), March 2014.
- [29] Juan Maldacena, Stephen H. Shenker, and Douglas Stanford. A bound on chaos. *Journal of High Energy Physics*, 2016(8), August 2016.
- [30] Yunxiang Liao and Victor Galitski. Nonlinear sigma model approach to many-body quantum chaos: Regularized and unregularized out-of-time-ordered correlators. *Phys. Rev. B*, 98:205124, Nov 2018.
- [31] Martin C. Gutzwiller. *Chaos in Classical and Quantum Mechanics*. Springer New York, NY, 1990.
- [32] Douglas Stanford. Many-body chaos at weak coupling. *Journal of High Energy Physics*, 2016(10), October 2016.

- [33] Aavishkar A. Patel, Debanjan Chowdhury, Subir Sachdev, and Brian Swingle. Quantum Butterfly Effect in Weakly Interacting Diffusive Metals. *Physical Review X*, 7(3), September 2017.
- [34] Bertrand Evrard, Andrea Pizzi, Simeon I. Mistakidis, and Ceren B. Dag. Quantum many-body scars from unstable periodic orbits. *Phys. Rev. B*, 110:144302, Oct 2024.
- [35] Andrea Pizzi, Bertrand Evrard, Ceren B. Dag, and Johannes Knolle. Quantum scars in many-body systems, 2024.
- [36] I-Chi Chen, Benjamin Burdick, Yongxin Yao, Peter P. Orth, and Thomas Iadecola. Error-mitigated simulation of quantum many-body scars on quantum computers with pulse-level control. *Phys. Rev. Res.*, 4:043027, Oct 2022.
- [37] Erik J. Gustafson, Andy C. Y. Li, Abid Khan, Joonho Kim, Doga Murat Kurkcuoglu, M. Sohaib Alam, Peter P. Orth, Armin Rahmani, and Thomas Iadecola. Preparing quantum many-body scar states on quantum computers. *Quantum*, 7:1171, November 2023.
- [38] Ivan Kukuljan, Sašo Grozdanov, and Tomaž Prosen. Weak quantum chaos. *Physical Review B*, 96(6), August 2017.